Stochastic Geometry

A toolbox for mathematical analysis, modeling and simulation of complex geometrical patterns on various length scales

Volker Schmidt

Ulm University, Institute of Stochastics

Paris, June 28th, 2013

Contents

Contents

Motivation/Goals

What is the benefit of stochastic network modeling?

Motivation/Goals

What is the benefit of stochastic network modeling?

- Representing the essential information of huge databases by a small number of model parameters

Motivation/Goals

What is the benefit of stochastic network modeling?

- Representing the essential information of huge databases by a small number of model parameters

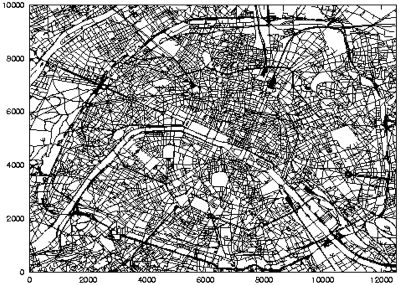

- road system of Paris city
- (real) geographical data set consisting of main roads and side streets

Motivation/Goals

What is the benefit of stochastic network modeling?

- Representing the essential information of huge databases by a small number of model parameters

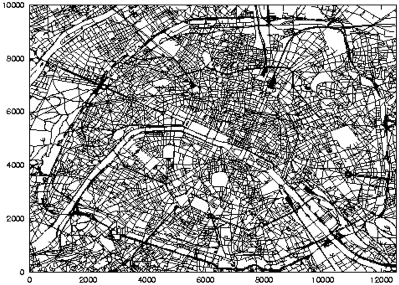

- road system of Paris city
- (real) geographical data set consisting of main roads and side streets

$\Rightarrow$ object-oriented modeling (grid-free, fast algorithms)

Motivation/Goals

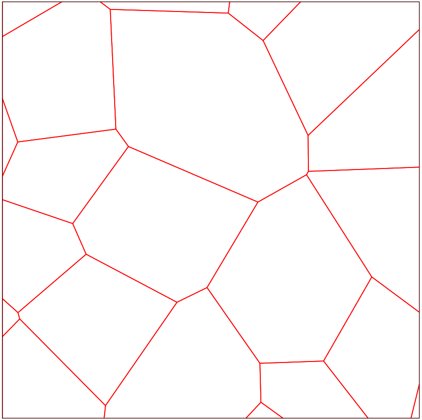

Simulated main roads

- Main roads

Motivation/Goals

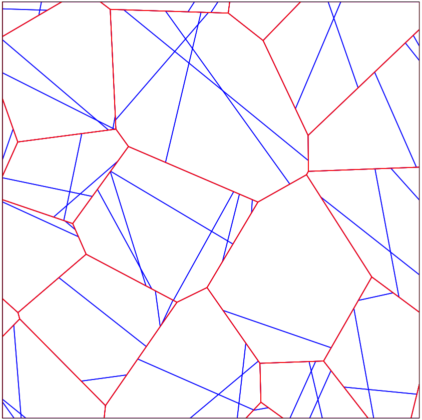

Simulated side streets

- Main roads
- Side streets

Motivation/Goals

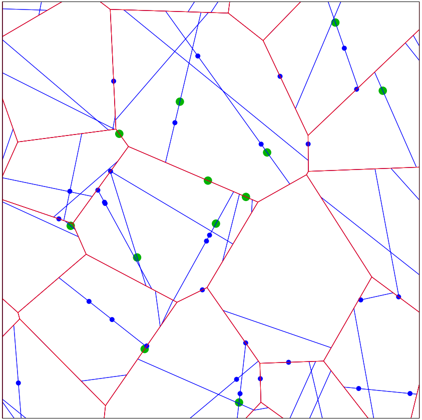

- Main roads
- Side streets
- Network components:
  - High-level components (green)
  - Low-level components (blue)

Network components along the roads/streets

Motivation/Goals

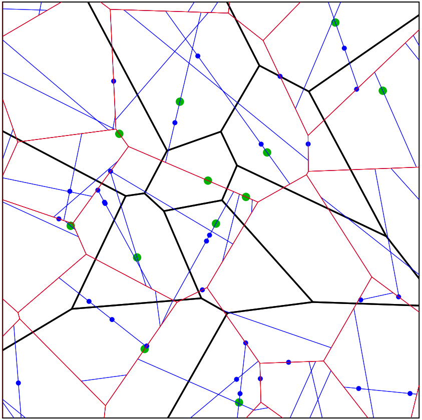

Serving zones

- Main roads
- Side streets
- Network components:
  - High-level components (green)
  - Low-level components (blue)
- Serving zones of high-level components (black)

Motivation/Goals

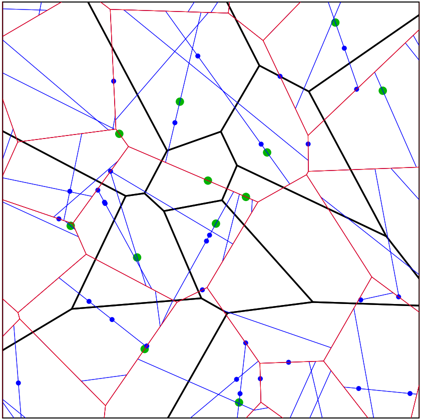

Serving zones

- Main roads
- Side streets
- Network components:
  - High-level components (green)
  - Low-level components (blue)
- Serving zones of high-level components (black)
- shortest-path tree in serving zones

Motivation/Goals

- developing a toolbox of stochastic network models ('to be kept in stock')

Motivation/Goals

- developing a toolbox of stochastic network models ('to be kept in stock')

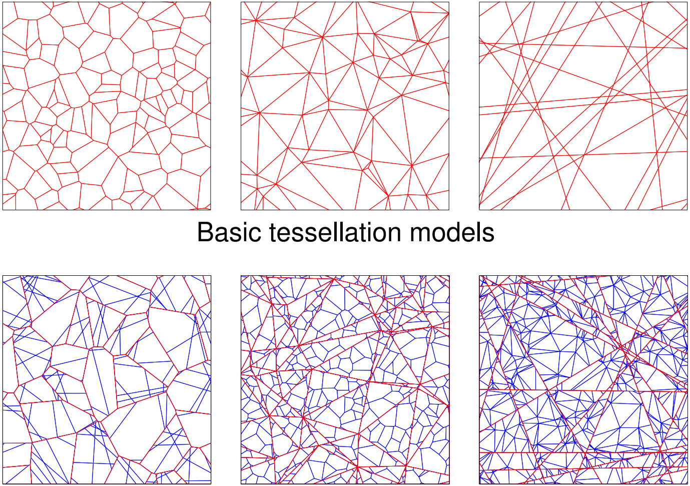

Basic tessellation models

Iterated tessellation models

Motivation/Goals

- using the 'model library' to investigate physical network properties (performance, costs) of existing **and** future networks

Motivation/Goals

- using the ’model library’ to investigate physical network properties (performance, costs) of existing **and** future networks

  $\Rightarrow$ virtual networks design on the computer

Motivation/Goals

- using the 'model library' to investigate physical network properties (performance, costs) of existing **and** future networks

  $\Rightarrow$ virtual networks design on the computer

  $\Rightarrow$ construction of (virtual) networks with improved/otimised properties

Motivation/Goals

- using the 'model library' to investigate physical network properties (performance, costs) of existing **and** future networks

  $\Rightarrow$ virtual networks design on the computer

  $\Rightarrow$ construction of (virtual) networks with improved/otimised properties

  $\Rightarrow$ computation of relevant network characteristics using extensive Monte Carlo simulations and (approximative) analytical formulas

Motivation/Goals

- using the 'model library' to investigate physical network properties (performance, costs) of existing **and** future networks

  $\Rightarrow$ virtual networks design on the computer

  $\Rightarrow$ construction of (virtual) networks with improved/otimised properties

  $\Rightarrow$ computation of relevant network characteristics using extensive Monte Carlo simulations and (approximative) analytical formulas

  $\Rightarrow$ establish quantitative (functional) relationships between
  - spatial distribution of infrastructure/network components and
  - network performance

Motivation/Goals

- using the 'model library' to investigate physical network properties (performance, costs) of existing **and** future networks

$\Rightarrow$ virtual networks design on the computer

$\Rightarrow$ construction of (virtual) networks with improved/otimised properties

$\Rightarrow$ computation of relevant network characteristics using extensive Monte Carlo simulations and (approximative) analytical formulas

$\Rightarrow$ establish quantitative (functional) relationships between

- spatial distribution of infrastructure/network components and
- network performance

$\Rightarrow$ combined modeling and simulation of

- spatial network structure and
- network transport/performance (transport-relevant cost functionals)

Contents

Overview

Models of stochastic geometry for

Overview

Models of stochastic geometry for

- two-dimensional patterns on geographical scales

Overview

Models of stochastic geometry for

- two-dimensional patterns on geographical scales

  $\Rightarrow$ telecommunication networks

  $\Rightarrow$ tropical cyclone tracks

Overview

Models of stochastic geometry for

- two-dimensional patterns on geographical scales

  $\Rightarrow$ telecommunication networks

  $\Rightarrow$ tropical cyclone tracks

- three-dimensional patterns on microscopic scales

Overview

Models of stochastic geometry for

- two-dimensional patterns on geographical scales

  $\Rightarrow$ telecommunication networks

  $\Rightarrow$ tropical cyclone tracks

- three-dimensional patterns on microscopic scales

  $\Rightarrow$ Li-ion batteries

  $\Rightarrow$ organic solar cells

  $\Rightarrow$ fuel cells

  $\Rightarrow$ polycristalline alloys

Contents

2D patterns on geographical scales

- telecommunication networks (inner-city, nationwide)
- tropical cyclone tracks

2D patterns on geographical scales

- **telecommunication networks (inner-city, nationwide)**
- tropical cyclone tracks

Stochastic modelling of network components

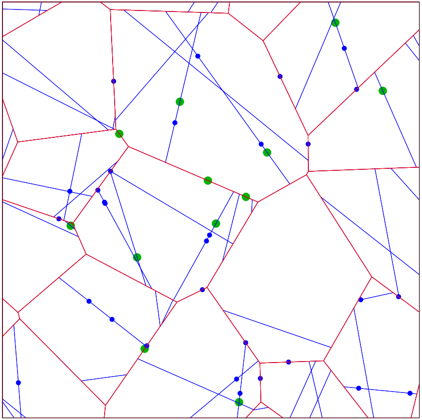

- Main roads and side streets modelled by stationary random graph T with length intensity $\gamma = \mathbb{E}\nu_1(T^{(1)} \cap [0,1]^2)$
- Network components:
  - High-level components: Cox process X_H with linear intensity λ_ℓ (HLC)
  - Low-level components: Cox process X_L with linear intensity λ'_ℓ (LLC)

Network components along the roads/streets

Stochastic modelling of serving zones

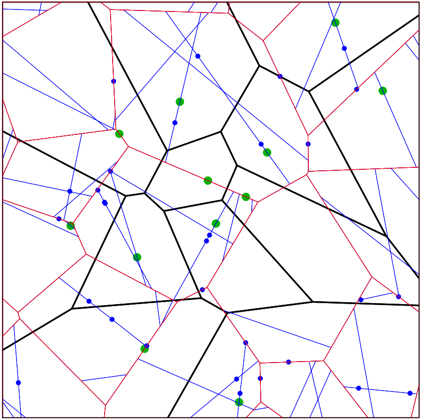

Serving zones

- Main roads and side streets modelled by stationary random graph T with length intensity $\gamma = \mathbb{E}\nu_1(T^{(1)} \cap [0,1]^2)$
- Network components:
  - High-level components: Cox process X_H with linear intensity λ_ℓ (HLC)
  - Low-level components: Cox process X_L with linear intensity λ'_ℓ (LLC)
- Serving zones of high-level components
  - to connect LLC to closest HLC

Stochastic modelling of serving zones

- consider the Voronoi tessellation $T_H = \{\Xi_{H,n}\}$ induced by the points $X_{H,n}$ of the Cox process $X_H = \{X_{H,n}\}$

Stochastic modelling of serving zones

- consider the Voronoi tessellation $T_H = \{\Xi_{H,n}\}$ induced by the points $X_{H,n}$ of the Cox process $X_H = \{X_{H,n}\}$
- i.e.,

$$\Xi_{H,n} = \{x \in \mathbb{R}^2 : |x - X_{H,n}| \leq |x - X_{H,m}| \text{ for all } m \neq n\}$$

Stochastic modelling of serving zones

- consider the Voronoi tessellation $T_H = \{\Xi_{H,n}\}$ induced by the points $X_{H,n}$ of the Cox process $X_H = \{X_{H,n}\}$
- i.e.,

$$\Xi_{H,n} = \{x \in \mathbb{R}^2 : |x - X_{H,n}| \leq |x - X_{H,m}| \text{ for all } m \neq n\}$$

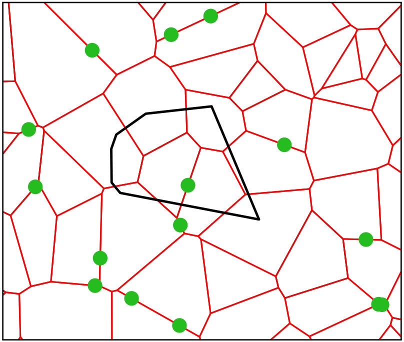

Cox-Voronoi cell

Shortest-path length

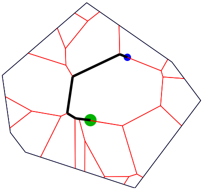

- Serving zone with shortest-path connection starting from an LLC and ending at the corresponding HLC

Shortest-path length

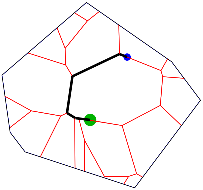

- Serving zone with shortest-path connection starting from an LLC and ending at the corresponding HLC
- distribution of shortest-path lengths depends both on λ_ℓ and γ

Shortest-path length

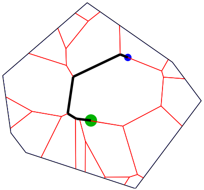

- Serving zone with shortest-path connection starting from an LLC and ending at the corresponding HLC
- distribution of shortest-path lengths depends both on λ_ℓ and γ
- however, for PVT, PLT and PDT we have a certain scaling invariance

Shortest-path length

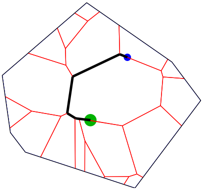

- Serving zone with shortest-path connection starting from an LLC and ending at the corresponding HLC
- distribution of shortest-path lengths depends both on λ_ℓ and γ
- however, for PVT, PLT and PDT we have a certain scaling invariance $\Rightarrow$ suffices to consider the ratio $\kappa = \frac{\gamma}{\lambda_\ell}$ called scaling parameter

Typical serving zone

- choose one of the serving zones at random $\Rightarrow$ typical serving zone

Typical serving zone

- choose one of the serving zones at random $\Rightarrow$ typical serving zone
- more formally, consider Palm version X_H^* of X_H whose distribution has representation formula

$$\mathbb{E} g(X_H^*) = \frac{1}{\lambda_H} \mathbb{E} \sum_{i:\, X_{H,i} \in [0,1]^2} g(\{X_{H,n}\} - X_{H,i}),$$

- where $g : \mathbb{L} \to [0, \infty)$ is an arbitrary measurable function and $\mathbb{L}$ denotes the family of all locally finite sets of $\mathbb{R}^2$

Typical serving zone

- choose one of the serving zones at random $\Rightarrow$ typical serving zone
- more formally, consider Palm version X_H^* of X_H whose distribution has representation formula

$$\mathbb{E}g(X_H^*) = \frac{1}{\lambda_H}\,\mathbb{E}\sum_{i:\,X_{H,i}\in[0,1]^2} g(\{X_{H,n}\} - X_{H,i})\,,$$

- where $g : \mathbb{L} \to [0,\infty)$ is an arbitrary measurable function and $\mathbb{L}$ denotes the family of all locally finite sets of $\mathbb{R}^2$
- typical serving zone $\Xi_H^* =$ cell associated with the cell centre o in the Voronoi tessellation constructed from X_H^*

Typical serving zone

- choose one of the serving zones at random $\Rightarrow$ typical serving zone
- more formally, consider Palm version X_H^* of X_H whose distribution has representation formula

$$\mathbb{E}g(X_H^*) = \frac{1}{\lambda_H}\,\mathbb{E}\sum_{i:\, X_{H,i}\in[0,1]^2} g(\{X_{H,n}\} - X_{H,i})\,,$$

- where $g : \mathbb{L} \to [0,\infty)$ is an arbitrary measurable function and $\mathbb{L}$ denotes the family of all locally finite sets of $\mathbb{R}^2$
- typical serving zone $\Xi_H^* =$ cell associated with the cell centre o in the Voronoi tessellation constructed from X_H^*
- i.e.,

$$\Xi_H^* = \{x \in \mathbb{R}^2 :\ \|x\| \leq \|x - X_{H,j}^*\| \ \text{ for all } j \geq 1\}$$

Shortest-path tree G on Ξ_H^*

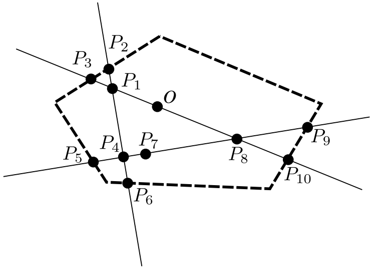

Typical serving zone Ξ_H^* (dashed) and corresponding segment system S_H^* (solid)

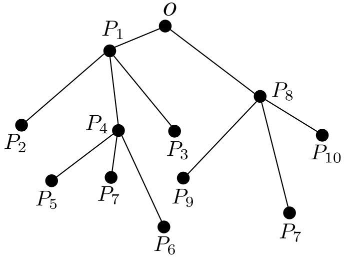

Shortest-path tree G with origin o as root

Shortest-path tree G on Ξ_H^*

- **Motivation:** engineers are mainly interested in minimising the total length of the telecommunication networks in a city

Shortest-path tree G on Ξ_H^*

- **Motivation:** engineers are mainly interested in minimising the total length of the telecommunication networks in a city
- **But:** further cost functionals have to be considered, e.g. capacity functionals

Shortest-path tree G on Ξ_H^*

- **Motivation:** engineers are mainly interested in minimising the total length of the telecommunication networks in a city
- **But:** further cost functionals have to be considered, e.g. capacity functionals
- **Idea:** consider the shortest-path tree from the typical serving zone

Shortest-path tree G on Ξ_H^*

- **Motivation:** engineers are mainly interested in minimising the total length of the telecommunication networks in a city
- **But:** further cost functionals have to be considered, e.g. capacity functionals
- **Idea:** consider the shortest-path tree from the typical serving zone
- closely related with capacity problems

Shortest-path tree G on Ξ_H^*

- **Motivation:** engineers are mainly interested in minimising the total length of the telecommunication networks in a city
- **But:** further cost functionals have to be considered, e.g. capacity functionals
- **Idea:** consider the shortest-path tree from the typical serving zone
- closely related with capacity problems
- and cost estimation for telecommunication networks

Main branches of G

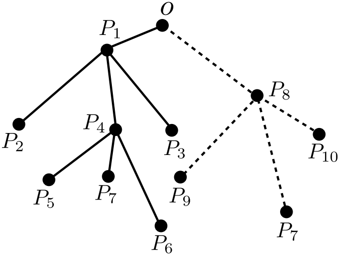

Half-trees G_1^h (solid) and G_2^h (dashed) of G emanating from the root

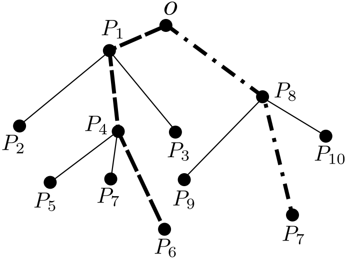

Main branches LSP (dashed) and LSP' (dot-dashed) of the corresponding half-trees

The idea of using copulas

- **Goal:** Find suitable parametric family of bivariate distributions for the lengths C_{LSP} and $C_{LSP'}$ of the two main branches LSP and LSP'

The idea of using copulas

- **Goal:** Find suitable parametric family of bivariate distributions for the lengths C_{LSP} and $C_{LSP'}$ of the two main branches LSP and LSP'
- **Problem:** it cannot be assumed that C_{LSP} and $C_{LSP'}$ are independent random variables

$$\Longrightarrow \quad F_{(C_{LSP},C_{LSP'})}(x,y) \neq F_{C_{LSP}}(x) \cdot F_{C_{LSP'}}(y)$$

The idea of using copulas

- **Goal:** Find suitable parametric family of bivariate distributions for the lengths C_{LSP} and $C_{LSP'}$ of the two main branches LSP and LSP'
- **Problem:** it cannot be assumed that C_{LSP} and $C_{LSP'}$ are independent random variables

$$\Longrightarrow \quad F_{(C_{LSP}, C_{LSP'})}(x, y) \neq F_{C_{LSP}}(x) \cdot F_{C_{LSP'}}(y)$$

- **Possible solution:** use a parametric copula combining marginal distributions to a joint distribution of $\mathbf{C} = (C_{LSP}, C_{LSP'})$

The idea of using copulas

- **Goal:** Find suitable parametric family of bivariate distributions for the lengths C_{LSP} and $C_{LSP'}$ of the two main branches LSP and LSP'
- **Problem:** it cannot be assumed that C_{LSP} and $C_{LSP'}$ are independent random variables

$$\Longrightarrow \quad F_{(C_{LSP}, C_{LSP'})}(x, y) \neq F_{C_{LSP}}(x) \cdot F_{C_{LSP'}}(y)$$

- **Possible solution:** use a parametric copula combining marginal distributions to a joint distribution of $\mathbf{C} = (C_{LSP}, C_{LSP'})$

Definition (bivariate copula)

A function $K : [0, 1]^2 \to [0, 1]$ is called a bivariate copula if there exists a probability space $(\Omega, \mathcal{F}, \mathbb{P})$ supporting a random vector $\mathbf{U} = (U_1, U_2)$ such that $U_i \sim U[0, 1]$ for $i \in \{1, 2\}$ and

$$K(u_1, u_2) = \mathbb{P}(U_1 \leq u_1, U_2 \leq u_2), \quad u_1, u_2 \in [0, 1]$$

The idea of using copulas

$\Longrightarrow$ the bivariate joint distribution function of the random vector $\mathbf{C} = (C_{LSP}, C_{LSP'})$ can be written as

$$F_{\mathbf{C}}(\mathbf{c}) = K_{\mathbf{C}}(F_{C_{LSP}}(c_1), F_{C_{LSP'}}(c_2))$$

where $\mathbf{c} = (c_1, c_2)$, $c_1, c_2 > 0$ (Sklar's theorem)

The idea of using copulas

$\Longrightarrow$ the bivariate joint distribution function of the random vector $\mathbf{C} = (C_{LSP}, C_{LSP'})$ can be written as

$$F_{\mathbf{C}}(\mathbf{c}) = K_{\mathbf{C}}(F_{C_{LSP}}(c_1), F_{C_{LSP'}}(c_2))$$

where $\mathbf{c} = (c_1, c_2)$, $c_1, c_2 > 0$ (Sklar's theorem)

Maximum-likelihood method (ML)

- assume parametric models for $F_{C_{LSP}}(\cdot \mid \boldsymbol{\eta}_1)$, $F_{C_{LSP'}}(\cdot \mid \boldsymbol{\eta}_2)$ and $K_{\mathbf{C}}(\cdot \mid \boldsymbol{\eta})$ with parameter vectors $\boldsymbol{\eta}_1$, $\boldsymbol{\eta}_2$ and $\boldsymbol{\eta}$

The idea of using copulas

$\Longrightarrow$ the bivariate joint distribution function of the random vector $\mathbf{C} = (C_{LSP}, C_{LSP'})$ can be written as

$$F_{\mathbf{C}}(\mathbf{c}) = K_{\mathbf{C}}(F_{C_{LSP}}(c_1), F_{C_{LSP'}}(c_2))$$

where $\mathbf{c} = (c_1, c_2)$, $c_1, c_2 > 0$ (Sklar's theorem)

Maximum-likelihood method (ML)

- assume parametric models for $F_{C_{LSP}}(\cdot \mid \boldsymbol{\eta}_1)$, $F_{C_{LSP'}}(\cdot \mid \boldsymbol{\eta}_2)$ and $K_{\mathbf{C}}(\cdot \mid \boldsymbol{\eta})$ with parameter vectors $\boldsymbol{\eta}_1$, $\boldsymbol{\eta}_2$ and $\boldsymbol{\eta}$
- for a sample $\mathbf{c}_i = (c_{LSP,i}, c_{LSP',i})$, $i = 1, \ldots, n$, consider the loglikelihood

$$\begin{aligned} \log L(\boldsymbol{\eta}_1\, \boldsymbol{\eta}_2, \boldsymbol{\eta}) &= \sum_{i=1}^{n} \Big(\log f_{C_{LSP}}(c_{LSP,i} \mid \boldsymbol{\eta}_1) + \log f_{C_{LSP'}}(c_{LSP',i} \mid \boldsymbol{\eta}_2) \\ &+ \log \left[k_{\mathbf{C}}(F_{C_{LSP}}(c_{LSP,i} \mid \boldsymbol{\eta}_1), F_{C_{LSP'}}(c_{LSP',i} \mid \boldsymbol{\eta}_2) \mid \boldsymbol{\eta})\right]\Big) \end{aligned}$$

2D patterns on geographical scales

- telecommunication networks (inner-city, nationwide)
- **tropical cyclone tracks**

Motivation

- Tropical cyclones are . . .
  - . . . major financial risk to (re-)insurance companies
  - . . . threat to human lives

Motivation

- Tropical cyclones are . . .
  - . . . major financial risk to (re-)insurance companies
  - . . . threat to human lives

- Examples
  - Hurricane Andrew, Florida, Louisiana, 1992: 26 fatalities, caused damages amounting to 25.5 billion U.S. Dollars
    $\rightarrow$ at this time costliest hurricane in U.S. history, 11 insurers went bankrupt
  - Hurricane Katrina, Florida, Louisiana, Mississippi, 2005: 1500 fatalities, caused damages amounting to 81 billion U.S. Dollars
    $\rightarrow$ costliest hurricane in U.S. history
  - Typhoon Mireille, Japan, 1991: 51 fatalities, caused damages amounting to 10 billion U.S. Dollars
    $\rightarrow$ costliest typhoon in the Western North Pacific

Motivation

- Tropical cyclones are ...
  - ... major financial risk to (re-)insurance companies
  - ... threat to human lives

- Examples
  - Hurricane Andrew, Florida, Louisiana, 1992: 26 fatalities, caused damages amounting to 25.5 billion U.S. Dollars
    $\rightarrow$ at this time costliest hurricane in U.S. history, 11 insurers went bankrupt
  - Hurricane Katrina, Florida, Louisiana, Mississippi, 2005: 1500 fatalities, caused damages amounting to 81 billion U.S. Dollars
    $\rightarrow$ costliest hurricane in U.S. history
  - Typhoon Mireille, Japan, 1991: 51 fatalities, caused damages amounting to 10 billion U.S. Dollars
    $\rightarrow$ costliest typhoon in the Western North Pacific

- Necessity to assess risks posed by cyclones as precisely as possible

Motivation

Andrew, the Miami area

Katrina, New Orleans

Aftermath of hurricanes Andrew and Katrina

Motivation

- Problems
  - reliable cyclone track data only given for about 100 years
  - insurers interested in risks caused by the largest cyclones having very small occurrence probability ($< 0.1\%$)
  - tropical storm could occur that is more intense or causes more damage than any historical measurement
    $\rightarrow$ this happened 1992 (Andrew) and 2005 (Katrina) in North Atlantic

Motivation

- Problems
  - reliable cyclone track data only given for about 100 years
  - insurers interested in risks caused by the largest cyclones having very small occurrence probability ($< 0.1\%$)
  - tropical storm could occur that is more intense or causes more damage than any historical measurement
    $\rightarrow$ this happened 1992 (Andrew) and 2005 (Katrina) in North Atlantic
- Approach
  - analyze historical storm observations
  - fit a spatial stochastic model
  - generate further, synthetic cyclone tracks via Monte Carlo simulation
  - perform risk assessment based on more comprehensive storm event sets

Motivation

- Problems
  - reliable cyclone track data only given for about 100 years
  - insurers interested in risks caused by the largest cyclones having very small occurrence probability ($< 0.1\%$)
  - tropical storm could occur that is more intense or causes more damage than any historical measurement
    $\rightarrow$ this happened 1992 (Andrew) and 2005 (Katrina) in North Atlantic
- Approach
  - analyze historical storm observations
  - fit a spatial stochastic model
  - generate further, synthetic cyclone tracks via Monte Carlo simulation
  - perform risk assessment based on more comprehensive storm event sets
- Motivation for development of a stochastic simulation model for tropical cyclone tracks
  $\rightarrow$ joint research project between Ulm University and Munich RE

Historical cyclone observations

- Consider two ocean basins: Western North Pacific (WNP) and North Atlantic (NA) since . . .
  - . . . they offer the most comprehensive historical cyclone data bases
  - . . . the most endangered coastal areas belong to these regions
    $\rightarrow$ high relevance for insurance companies

Historical cyclone observations

- Consider two ocean basins: Western North Pacific (WNP) and North Atlantic (NA) since . . .
  - . . . they offer the most comprehensive historical cyclone data bases
  - . . . the most endangered coastal areas belong to these regions
    $\rightarrow$ high relevance for insurance companies

- Historical cyclone tracks are observed in 6 hours time intervals
  $\rightarrow$ the time, the geographical coordinates (storm location) and the maximum sustained wind speed are measured every 6 hours

Historical cyclone observations

- Consider two ocean basins: Western North Pacific (WNP) and North Atlantic (NA) since ...
  - ... they offer the most comprehensive historical cyclone data bases
  - ... the most endangered coastal areas belong to these regions
    $\rightarrow$ high relevance for insurance companies

- Historical cyclone tracks are observed in 6 hours time intervals
  $\rightarrow$ the time, the geographical coordinates (storm location) and the maximum sustained wind speed are measured every 6 hours

- Storm track is modeled as polygonal line by connecting each two successive storm locations

Historical cyclone observations

- Consider two ocean basins: Western North Pacific (WNP) and North Atlantic (NA) since ...
  - ... they offer the most comprehensive historical cyclone data bases
  - ... the most endangered coastal areas belong to these regions $\rightarrow$ high relevance for insurance companies
- Historical cyclone tracks are observed in 6 hours time intervals $\rightarrow$ the time, the geographical coordinates (storm location) and the maximum sustained wind speed are measured every 6 hours
- Storm track is modeled as polygonal line by connecting each two successive storm locations
- Additionally, translational speed and movement direction along each storm segment can be computed $\rightarrow$ both characteristics suffice to completely determine the pathway of a storm track

Historical cyclone observations - NA

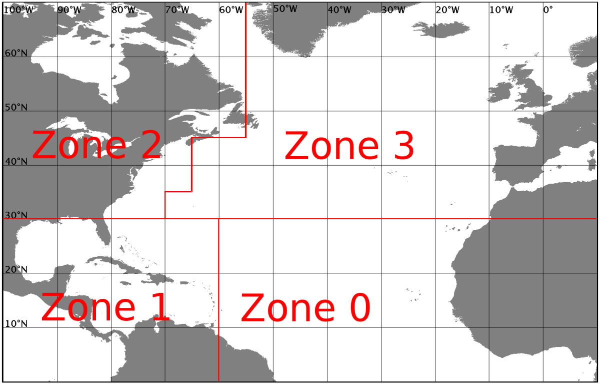

Observation window of the NA split into 4 zones

Historical cyclone observations - NA

- Criteria for the classification of cyclone tracks in the NA

start in zone	touched zones	end in zone	class
0	0	0	0
1	1	1	5
2	2	2	2
3	3	3	3
0	0 and 1	0	0
1	0 and 1	0	1
0	0 and 1	1	1
1	0 and 1	1	1
0 or 3	0 and 3	0 or 3	3
1	1 and 2	1	1
1 or 2	1 and 2	2	2
2	1 and 2	1	2
1 or 3	1 and 3	1 or 3	4
2 or 3	2 and 3	2 or 3	4
0	0, 1 and 2	0	0
1 or 2	0, 1 and 2	0	2

start in zone	touched zones	end in zone	class
0 or 1	0, 1 and 2	1	1
2	0, 1 and 2	1	2
0, 1, or 2	0, 1 and 2	2	2
0	0, 1 and 3	0	0
1 or 3	0, 1 and 3	0	3
0, 1 or 3	0, 1 and 3	1	1
0, 1 or 3	0, 1 and 3	3	3
0, 2 or 3	0, 2 and 3	0, 2 or 3	2
2	1, 2 and 3	1, 2 or 3	2
1 or 3	1, 2 and 3	1	1
1 or 3	1, 2 and 3	2 or 3	2
0	0, 1, 2 and 3	0	0
1, 2 or 3	0, 1, 2 and 3	0	2
1	0, 1, 2 and 3	1	1
0, 2 or 3	0, 1, 2 and 3	1	2
0, 1, 2 or 3	0, 1, 2 and 3	2 or 3	2

- Some cyclones that have been sorted into class 1 and satisfy certain conditions are moved to class 4 or 5

Historical cyclone observations - NA

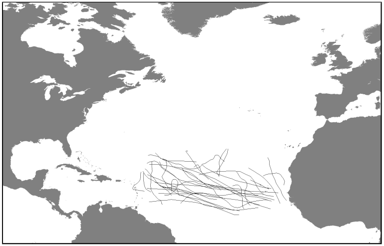

Historical cyclone tracks of class 0

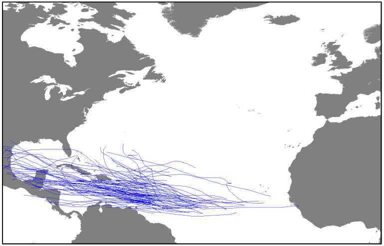

Historical cyclone tracks of class 1

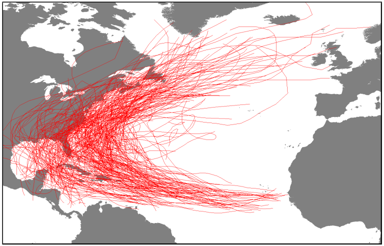

Historical cyclone tracks of class 2

Historical cyclone observations - NA

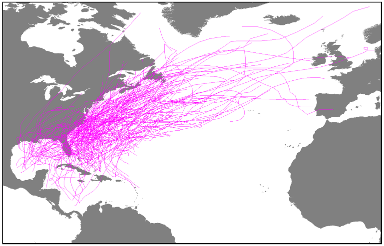

Historical cyclone tracks of class 4

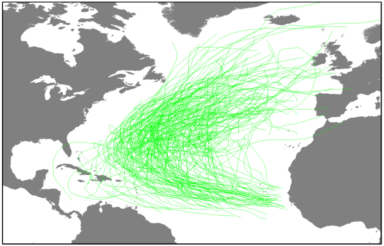

Historical cyclone tracks of class 3

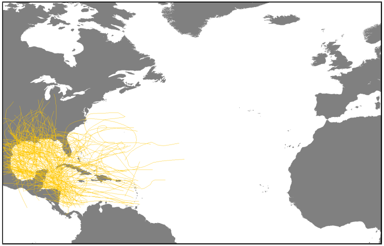

Historical cyclone tracks of class 5

UU/MR simulator

- UU/MR simulator for tropical cyclone tracks has been developed in a research cooperation between Ulm University and Munich RE

UU/MR simulator

- UU/MR simulator for tropical cyclone tracks has been developed in a research cooperation between Ulm University and Munich RE
- Storm event sets representing any arbitrary time span T can be generated,
  where typically $T \geq T_{hist}$
- Simulation is performed separately for each storm class

UU/MR simulator

- UU/MR simulator for tropical cyclone tracks has been developed in a research cooperation between Ulm University and Munich RE
- Storm event sets representing any arbitrary time span T can be generated,
  where typically $T \geq T_{hist}$
- Simulation is performed separately for each storm class
- Synthetic storms are modeled as polygonal lines, where each line segment represents movement of the storm during 6 hours

UU/MR simulator

- UU/MR simulator for tropical cyclone tracks has been developed in a research cooperation between Ulm University and Munich RE

- Storm event sets representing any arbitrary time span T can be generated,
  where typically $T \geq T_{hist}$

- Simulation is performed separately for each storm class

- Synthetic storms are modeled as polygonal lines, where each line segment represents movement of the storm during 6 hours

- Stochastic simulation model includes the following components:
  - model for points of storm genesis
  - track propagation (including maximum sustained wind speeds)
  - termination of cyclone tracks

Poisson point processes in $\mathbb{R}$

- Let $\mu : \mathcal{B} \to [0, \infty]$ be an arbitrary locally finite and diffuse measure

Poisson point processes in $\mathbb{R}$

- Let $\mu : \mathcal{B} \to [0, \infty]$ be an arbitrary locally finite and diffuse measure
- The family of random variables $\Phi = \{\Phi_B, B \in \mathcal{B}\}$ is called a Poisson process with intensity measure μ if (Stoyan *et al.* (1995))
  - $\Phi_{B_1}, \Phi_{B_2}, \ldots$ are independent random variables for all $B_1, B_2, \ldots \in \mathcal{B}_0(\mathbb{R}^d)$ pairwise disjoint
  - $\Phi_B \sim \text{Poi}(\mu(B))$ for each $B \in \mathcal{B}_0(\mathbb{R}^d)$

Poisson point processes in $\mathbb{R}$

- Let $\mu : \mathcal{B} \to [0, \infty]$ be an arbitrary locally finite and diffuse measure
- The family of random variables $\Phi = \{\Phi_B, B \in \mathcal{B}\}$ is called a Poisson process with intensity measure μ if (Stoyan *et al.* (1995))
  - $\Phi_{B_1}, \Phi_{B_2}, \dots$ are independent random variables for all $B_1, B_2, \dots \in \mathcal{B}_0(\mathbb{R}^d)$ pairwise disjoint
  - $\Phi_B \sim \mathrm{Poi}(\mu(B))$ for each $B \in \mathcal{B}_0(\mathbb{R}^d)$
- Assumption: μ is absolutely continuous, i.e. Φ has an intensity function $\lambda : \mathbb{R} \to [0, \infty)$ such that

$$\mu(B) = \int_B \lambda(x)\, dx \qquad \text{for all } \; B \in \mathcal{B}$$

$\to \lambda$ completely determines the distribution of Φ

Poisson point processes in $\mathbb{R}$

- Let $\mu : \mathcal{B} \to [0, \infty]$ be an arbitrary locally finite and diffuse measure
- The family of random variables $\Phi = \{\Phi_B, B \in \mathcal{B}\}$ is called a Poisson process with intensity measure μ if (Stoyan *et al.* (1995))
  - $\Phi_{B_1}, \Phi_{B_2}, \ldots$ are independent random variables for all $B_1, B_2, \ldots \in \mathcal{B}_0(\mathbb{R}^d)$ pairwise disjoint
  - $\Phi_B \sim \text{Poi}(\mu(B))$ for each $B \in \mathcal{B}_0(\mathbb{R}^d)$
- Assumption: μ is absolutely continuous, i.e. Φ has an intensity function $\lambda : \mathbb{R} \to [0, \infty)$ such that

$$\mu(B) = \int_B \lambda(x)\, dx \qquad \text{for all } B \in \mathcal{B}$$

  $\to \lambda$ completely determines the distribution of Φ

- Φ can be considered as random counting measure $\to$ there is a sequence of random vectors $S_1, S_2, \ldots$ in $\mathbb{R}$ such that $\Phi_B = \#\{i : S_i \in B\}$, $B \in \mathcal{B}$

Points of genesis

- The estimator $\hat{\lambda}$ for the intensity function λ is given by a generalized nearest-neighbor estimator, i.e.

$$\hat{\lambda}(x) = \frac{1}{r_k(x)^2} \sum_{i=1}^{n} K\left(\frac{S_i - x}{r_k(x)}\right) \qquad \text{for } x \in \mathbb{R}^2,$$

where

  - $S_1, \ldots, S_n$: starting points of historical cyclone observations
  - kernel function K: Epanechnikov kernel

$$K(x) = \begin{cases} \frac{2}{\pi}(1 - x^\top x) & \text{if } x^\top x < 1, \\ 0 & \text{else} \end{cases}$$

  - $r_k(x)$: distance from x to k-th nearest starting point
  - $k = \lfloor \sqrt{n} \rfloor$

Points of genesis - WNP

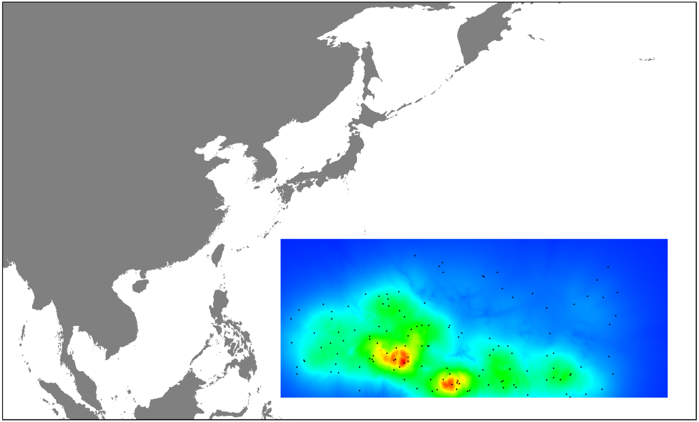

Starting points of historical storm tracks for class 0 in the WNP together with the estimated intensity function

Points of genesis - NA

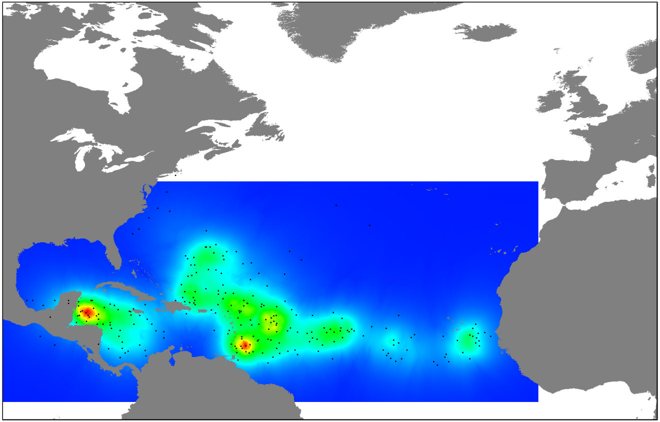

Starting points of historical storm tracks for class 2 in the NA together with the estimated intensity function

Track propagation

- Appropriate cyclone track model needs to include the direction of movement X and the translational speed Y

Track propagation

- Appropriate cyclone track model needs to include the direction of movement X and the translational speed Y
- Assume both characteristics to be constant for intervals of 6 hours and update $(X, Y)^\top$ after each of these intervals
  $\rightarrow$ the cyclone's location can be calculated in 6-hour steps
  $\rightarrow$ connecting these storm points yields a polygonal line

Track propagation

- Appropriate cyclone track model needs to include the direction of movement X and the translational speed Y
- Assume both characteristics to be constant for intervals of 6 hours and update $(X, Y)^\top$ after each of these intervals
  $\rightarrow$ the cyclone's location can be calculated in 6-hour steps
  $\rightarrow$ connecting these storm points yields a polygonal line
- Additionally, for risk assessment purposes at each storm point the maximum wind speed Z is considered

Track propagation

- Appropriate cyclone track model needs to include the direction of movement X and the translational speed Y
- Assume both characteristics to be constant for intervals of 6 hours and update $(X, Y)^\top$ after each of these intervals
  $\rightarrow$ the cyclone's location can be calculated in 6-hour steps
  $\rightarrow$ connecting these storm points yields a polygonal line
- Additionally, for risk assessment purposes at each storm point the maximum wind speed Z is considered
- The characteristics X_i, Y_i and Z_i after the i-th track segment are considered to be sums of initial values and the changes in these values after each step

$$\begin{pmatrix} X_i \\ Y_i \\ Z_i \end{pmatrix} = \begin{pmatrix} X_0 \\ Y_0 \\ Z_0 \end{pmatrix} + \sum_{j=1}^{i} \begin{pmatrix} \Delta X_j \\ \Delta Y_j \\ \Delta Z_j \end{pmatrix}$$

Track propagation

Track propagation

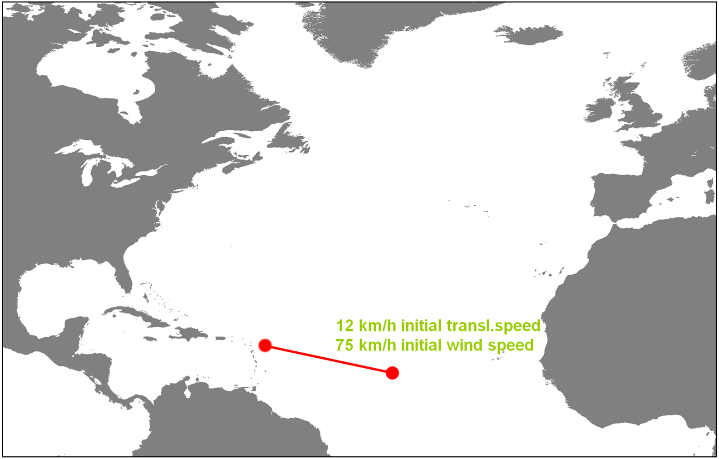

Track propagation

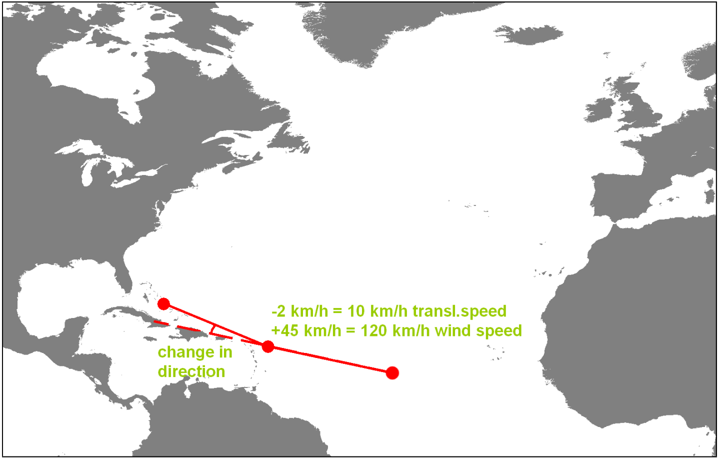

Track propagation

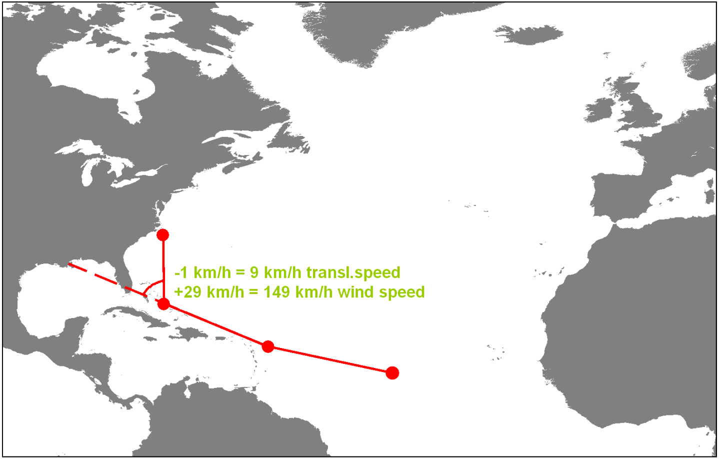

Track propagation

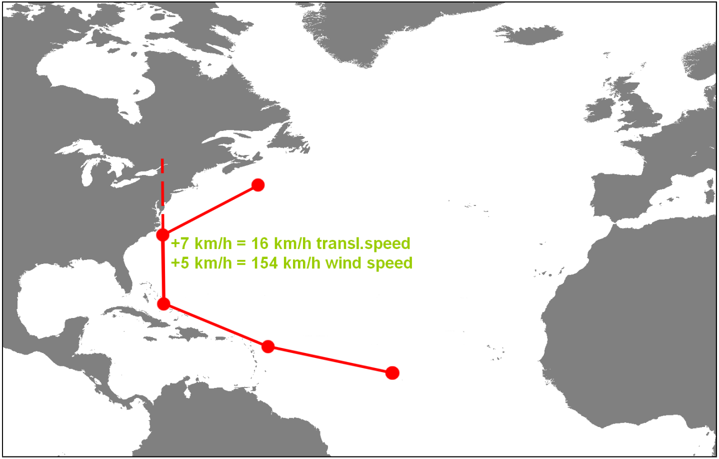

Track propagation

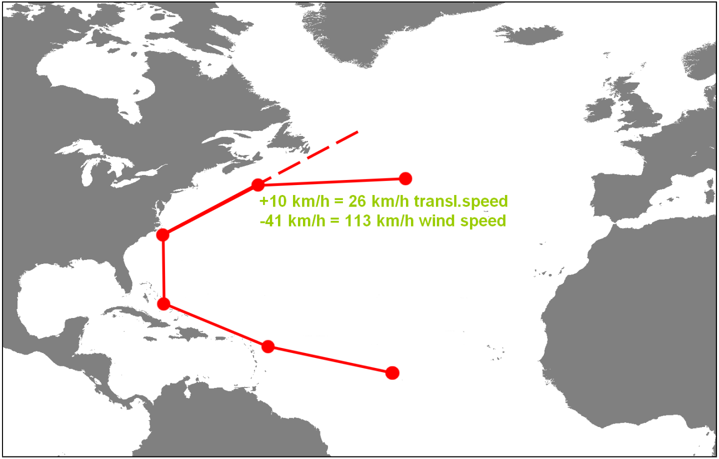

Track propagation

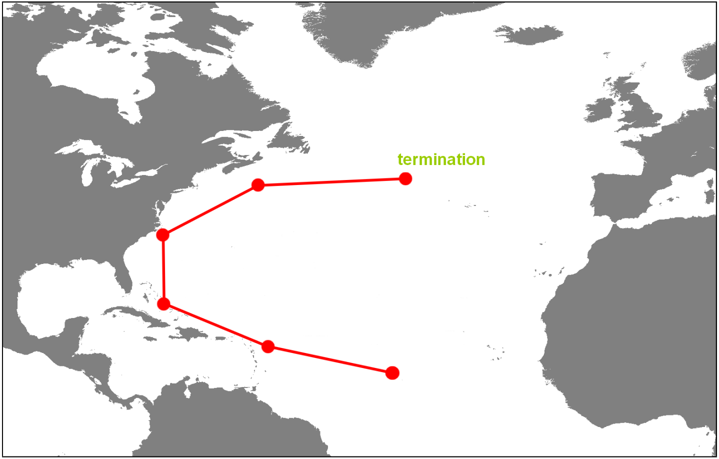

Comparison of cyclone tracks - NA

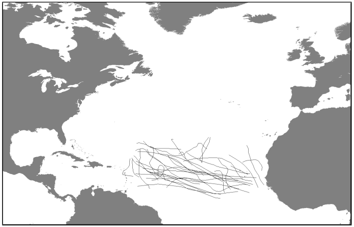

Historical cyclone tracks of class 0

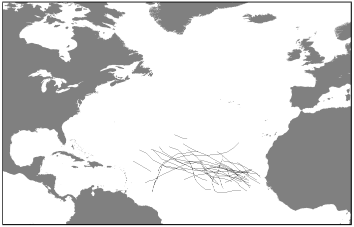

Simulated cyclone tracks of class 0

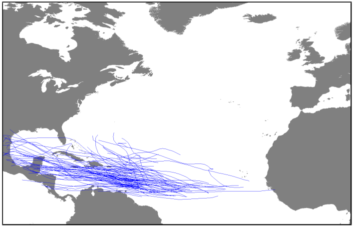

Historical cyclone tracks of class 1

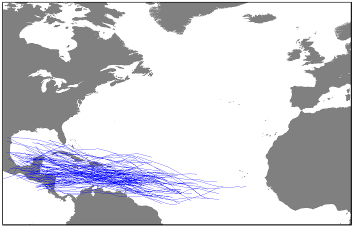

Simulated cyclone tracks of class 1

Comparison of cyclone tracks - NA

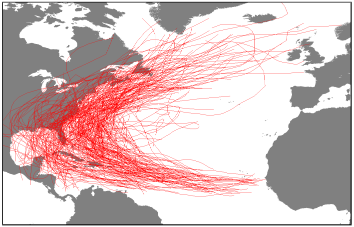

Historical cyclone tracks of class 2

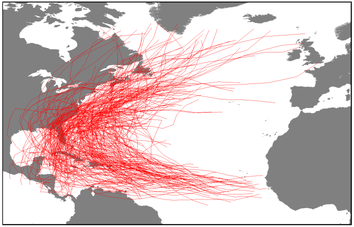

Simulated cyclone tracks of class 2

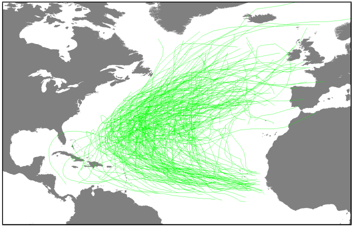

Historical cyclone tracks of class 3

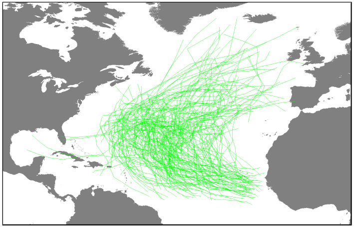

Simulated cyclone tracks of class 3

Comparison of cyclone tracks - NA

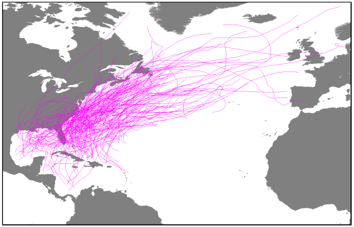

Historical cyclone tracks of class 4

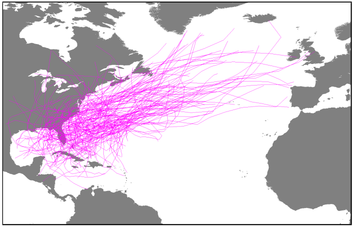

Simulated cyclone tracks of class 4

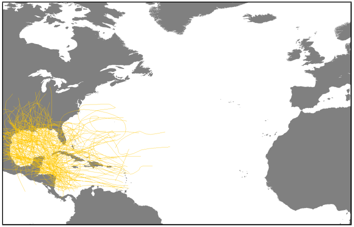

Historical cyclone tracks of class 5

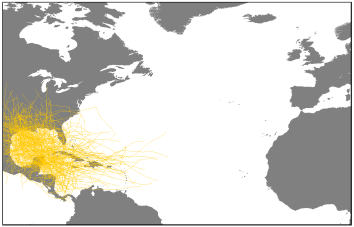

Simulated cyclone tracks of class 5

Validation - NA - hazard maps

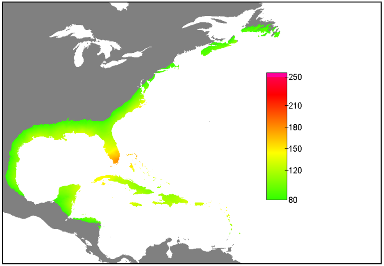

Historical

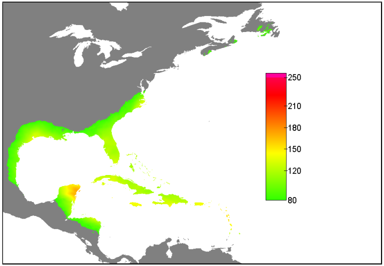

Simulated

Estimated hazard maps for storm event sets representing a time span of $T_{hist} = 111$ years
return period 5 years

Validation - NA - hazard maps

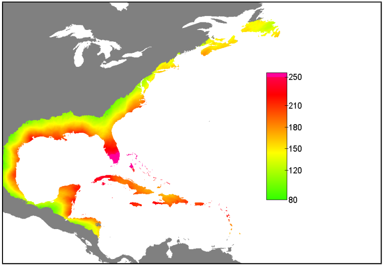

Historical

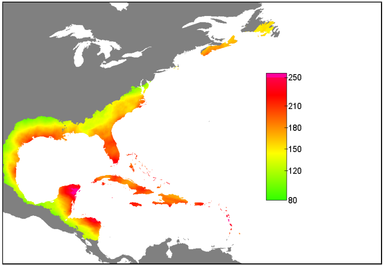

Simulated

Estimated hazard maps for storm event sets representing a time span of $T_{hist} = 111$ years
return period 25 years

Validation - NA - hazard maps

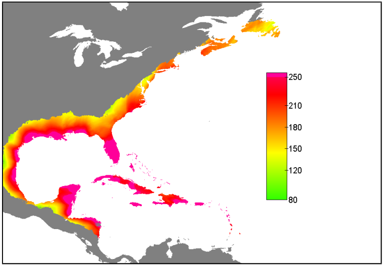

Historical

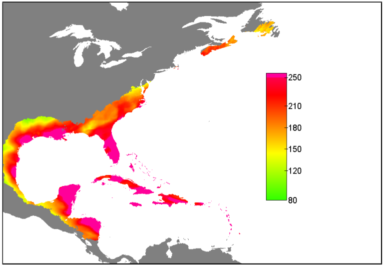

Simulated

Estimated hazard maps for storm event sets representing a time span of $T_{hist} = 111$ years
return period 100 years

Validation - NA - hazard maps

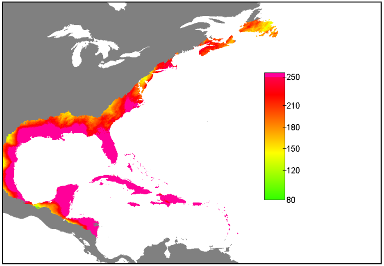

Historical

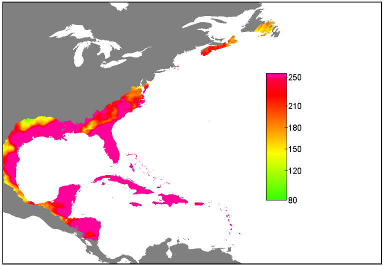

Simulated

Estimated hazard maps for storm event sets representing a time span of $T_{hist} = 111$ years
return period 500 years

Contents

3D patterns on microscopic scales

- Li-ion batteries
- organic solar cells
- fuel cells
- polycristalline alloys

3D patterns on microscopic scales

- **Li-ion batteries**
- organic solar cells
- fuel cells
- polycristalline alloys

Synchrotron tomography image data

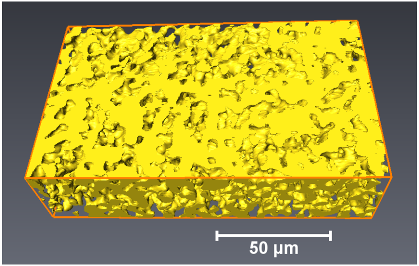

Synchrotron tomography image data

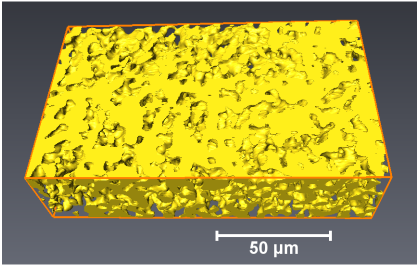

- 3D image of uncompressed graphite electrode used in Li-ion batteries
- tomography: Helmholtz Center Berlin, material: ZSW Baden-Württemberg
- yellow: graphite phase
- transparent: pore phase, volume fraction ca. 56%

Goal: stochastic simulation model

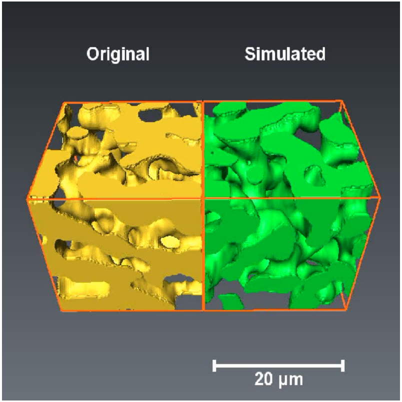

- Modeling of the 3D morphology of graphite electrodes
- Size: $100 \times 100 \times 100$ voxels

Functionality

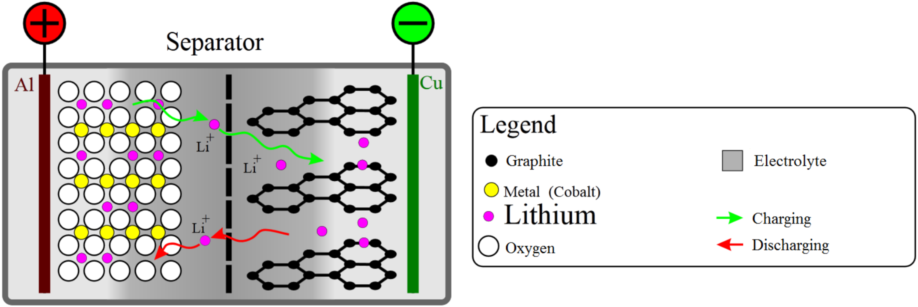

- 3D microstructure ⇔ functionality
- Detect improved microstructures by virtual materials design

Simulated annealing for generation of microstructures

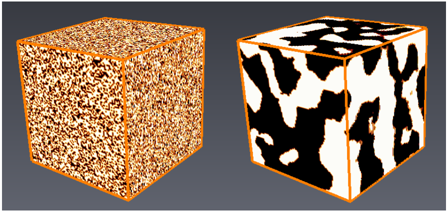

Simulated annealing for generation of microstructures

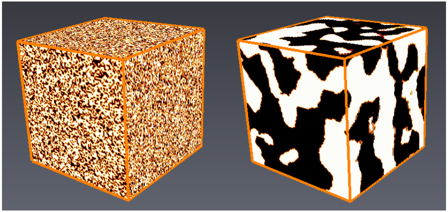

- Start with random allocation of voxels given volume fraction α

Simulated annealing for generation of microstructures

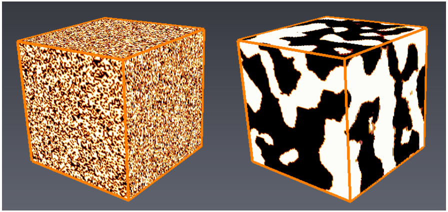

- Start with random allocation of voxels given volume fraction α
- Coarsening of morphology by interchanging voxels.
  - T temperature, $c(\cdot)$ cost function to be reduced (e.g. surface area)
  - Pick a pair of voxels at random
  - Swap voxels if cost function decreases, otherwise accept swap with probability $\exp\left(\frac{c(\text{no change}) - c(\text{change})}{T}\right)$
  - Decrease T with time

Simulated annealing for generation of microstructures

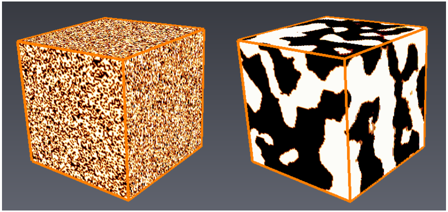

- Start with random allocation of voxels given volume fraction α
- Coarsening of morphology by interchanging voxels.
  - T temperature, $c(\cdot)$ cost function to be reduced (e.g. surface area)
  - Pick a pair of voxels at random
  - Swap voxels if cost function decreases, otherwise accept swap with probability $\exp\left(\frac{c(\text{no change}) - c(\text{change})}{T}\right)$
  - Decrease T with time
- Stop if desired value of $c(\cdot)$ is reached.

Our approach: graph-based simulated annealing

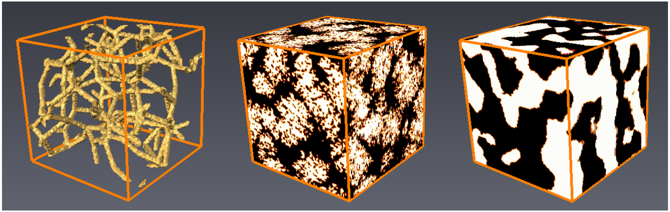

- Simulated annealing: simple but computational expensive, limited control of microstructure

Our approach: graph-based simulated annealing

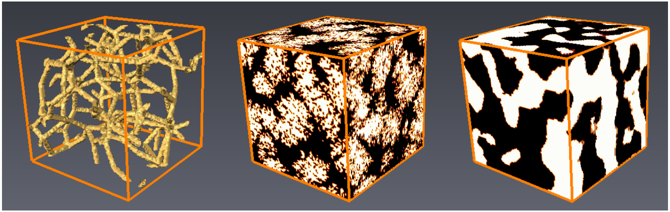

- Simulated annealing: simple but computational expensive, limited control of microstructure
- Hybrid approach: combining spatial stochastic graph modeling with simulated annealing
  - simulate random geometric graph
  - start configuration of voxels by project voxels onto the graph
  - run simulated annealing on new start configurations
  - voxels of graph fixed

Our approach: graph-based simulated annealing

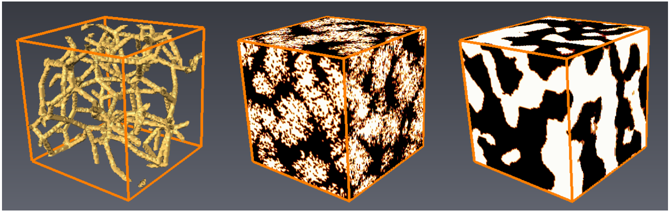

- Simulated annealing: simple but computational expensive, limited control of microstructure
- Hybrid approach: combining spatial stochastic graph modeling with simulated annealing
  - simulate random geometric graph
  - start configuration of voxels by project voxels onto the graph
  - run simulated annealing on new start configurations
  - voxels of graph fixed
- spatial graph serves as backbone of microstructure

Our approach: graph-based simulated annealing

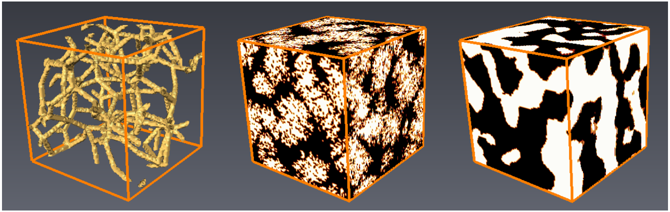

- Simulated annealing: simple but computational expensive, limited control of microstructure
- Hybrid approach: combining spatial stochastic graph modeling with simulated annealing
  - simulate random geometric graph
  - start configuration of voxels by project voxels onto the graph
  - run simulated annealing on new start configurations
  - voxels of graph fixed
- spatial graph serves as backbone of microstructure
- fast, good control on microstructure

Stochastic graph model

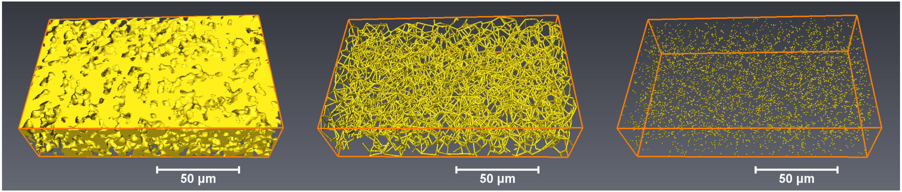

Stochastic graph model

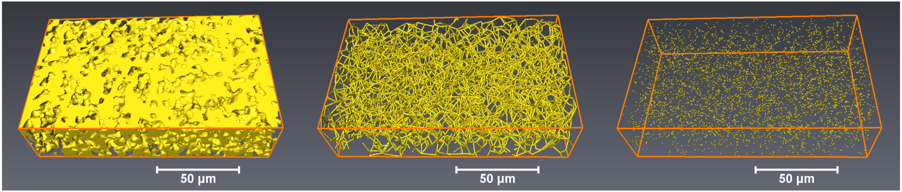

- Extract spatial graph (V, E) from experimental data by skeletonization
  - V set of vertices
  - E set of edges

Stochastic graph model

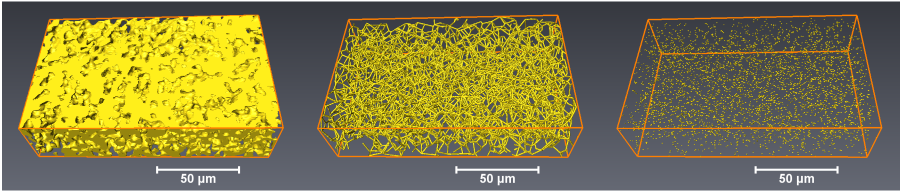

- Extract spatial graph (V, E) from experimental data by skeletonization
  - V set of vertices
  - E set of edges
- Stochastic modeling by
  - Point process model for the set of vertices
  - a stochastic model for setting edges
  - Fitting of model parameters to corresponding experimental data

Point process model: modulated hardcore point process

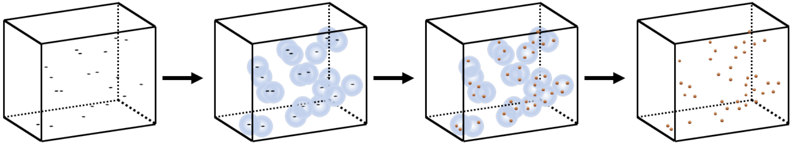

(1) Simulation of homogeneous Poisson process

Point process model: modulated hardcore point process

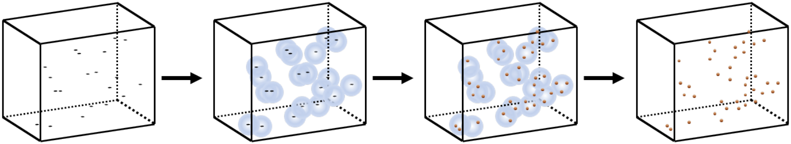

(1) Simulation of homogeneous Poisson process

(2) Simulation of Boolean Model

Point process model: modulated hardcore point process

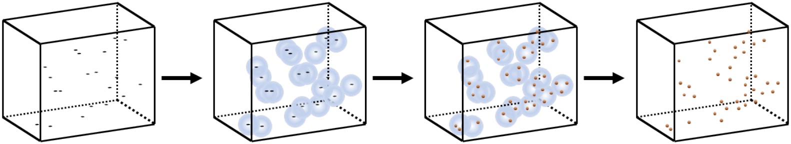

(1) Simulation of homogeneous Poisson process

(2) Simulation of Boolean Model

(3) Simulation of Poisson hardcore model inside the Boolean Model

Stochastic model for setting edges

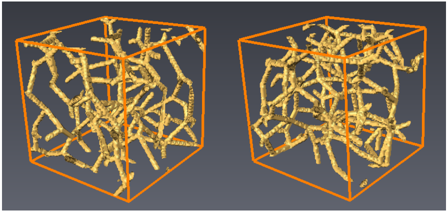

Cut-out of experimental graph (left) and simulated graph (right)

Stochastic model for setting edges

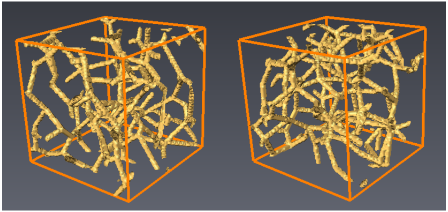

Cut-out of experimental graph (left) and simulated graph (right)

- Connecting nearest neighbors
  - Connect each point S_i with its n nearest neighbors.
  - Start with nearest neighbor
  - Connection is rejected if angle to previous edges undercuts a threshold γ_1

Stochastic model for setting edges

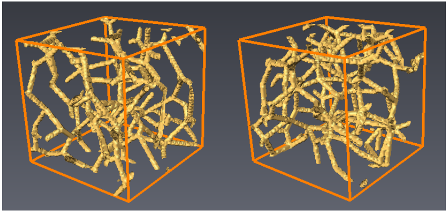

Cut-out of experimental graph (left) and simulated graph (right)

- Connecting nearest neighbors
  - Connect each point S_i with its n nearest neighbors.
  - Start with nearest neighbor
  - Connection is rejected if angle to previous edges undercuts a threshold γ_1
- Postprocessing of edges
  - If angles undercut threshold γ_2: deletion with probability $p \in (0, 1)$.
  - Control of angles

Model validation

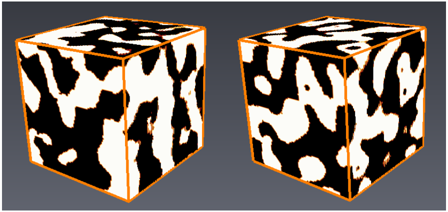

Cut-out of experimental (left) and simulated (right) microstructure

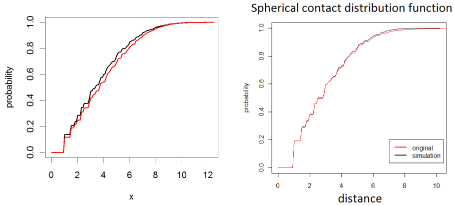

Spherical contact distribution from pore phase to graphite (left) and vice versa (right). Red curve displays experimental data and black curve simulated data.

3D patterns on microscopic scales

- Li-ion batteries
- **organic solar cells**
- fuel cells
- polycristalline alloys

Tomographic solar cell data

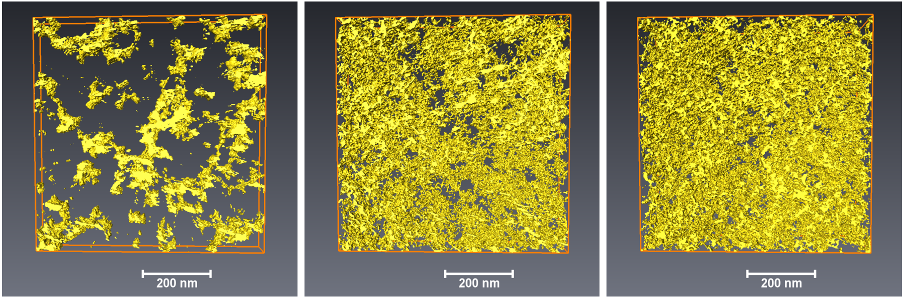

5000 rpm ∼ 57 nm 1500 rpm ∼ 100 nm 1000 rpm ∼ 167 nm

- 3D TEM images of P3HT-ZnO solar cells with different thicknesses
- TEM: Technical University Eindhoven
- P3HT-phase: transparent
- ZnO-phase: yellow, volume fraction 13.3% – 21.1%
- Morphology is anisotropic

Goal: stochastic simulation model

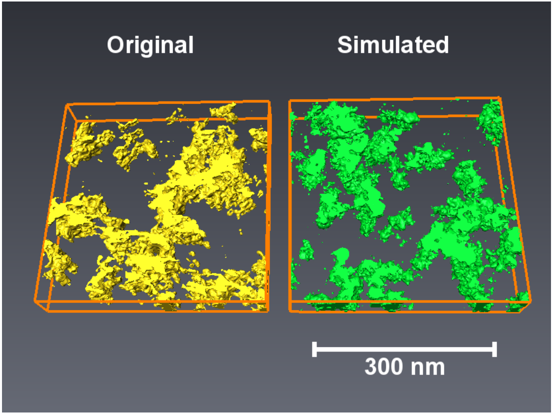

- same model type for all layer thicknesses
- different model parameters for different layer thicknesses

Functionality

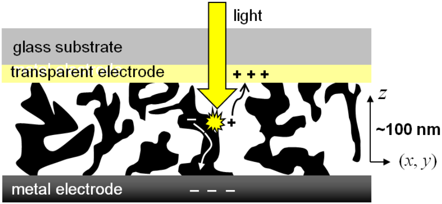

- Device architecture: bulk heterojunction
- Light acitivates the polymer phase of the solar cell

Functionality

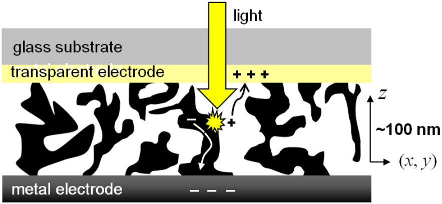

- Device architecture: bulk heterojunction
- Light acitivates the polymer phase of the solar cell
- Excitons are generated

Functionality

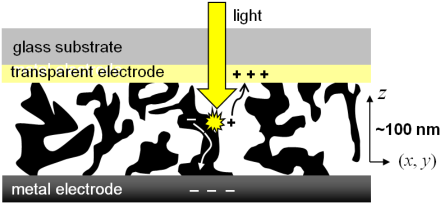

- Device architecture: bulk heterojunction
- Light acitivates the polymer phase of the solar cell
- Excitons are generated
- Diffusion of excitons in the polymer phase

Functionality

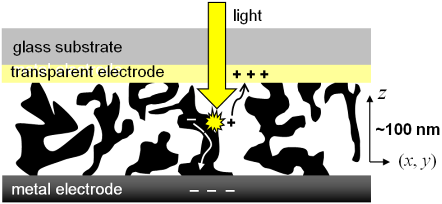

- Device architecture: bulk heterojunction
- Light acitivates the polymer phase of the solar cell
- Excitons are generated
- Diffusion of excitons in the polymer phase
- Excitons reaching the ZnO phase generate charges: quenching

Functionality

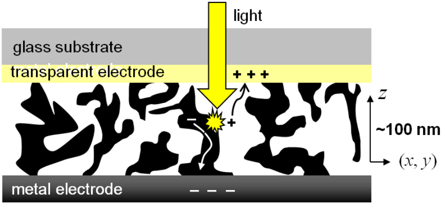

- Device architecture: bulk heterojunction
- Light acitivates the polymer phase of the solar cell
- Excitons are generated
- Diffusion of excitons in the polymer phase
- Excitons reaching the ZnO phase generate charges: quenching
- Transportation of charges to the electrodes
- 3D microstructure ⇔ functionality
- Detect improved microstructures by virtual materials design

Modeling idea: 'smart' system of spheres

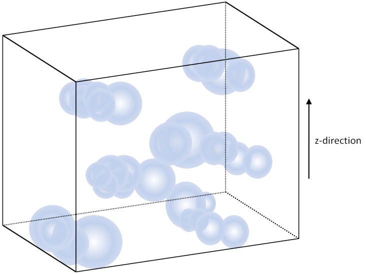

- Representation of the ZnO phase as a complex system of spheres
- Contrast to compressed battery modeling: anisotropic point pattern
- Anisotropy by Markov chain of 2D point processes

Multi-scale approach

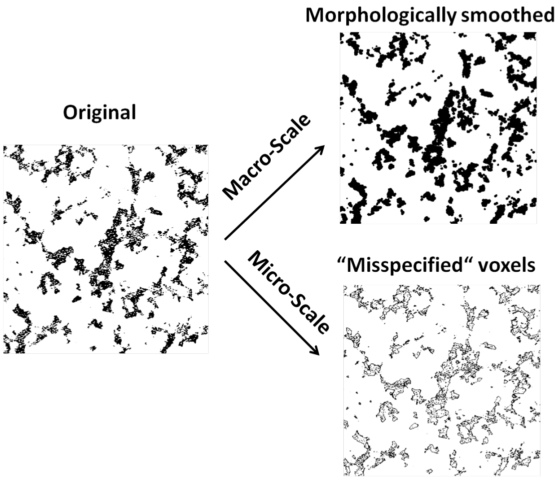

3D Representation of the macro-scale by unions of spheres

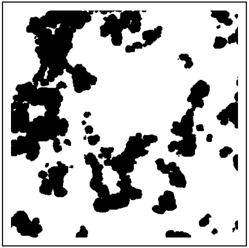

$\Longrightarrow$

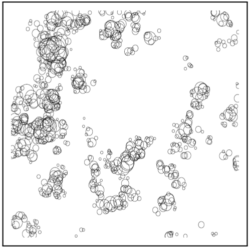

$$= \bigcup_{i=1}^{n} b(s_i, r_i)$$

- Macro-scale represented by marked point process
- Transformation of solar cells into mathematical language

Modeling in 2 steps:

- 2D point patterns: elliptical Matérn cluster process
- 3D stack of 2D point patterns: spatial birth-and-death process

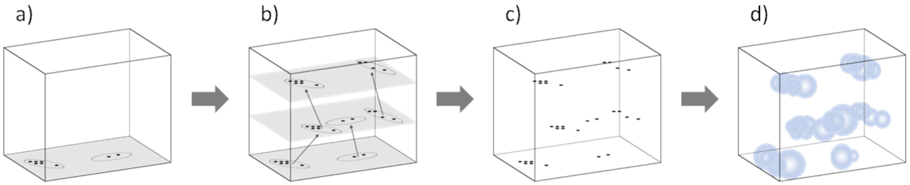

Inversion of morphological smoothing by stochastic modeling

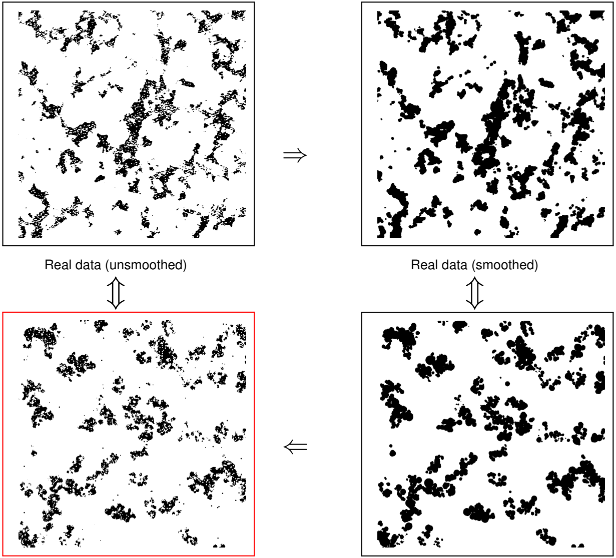

Result: stochastic simulation model

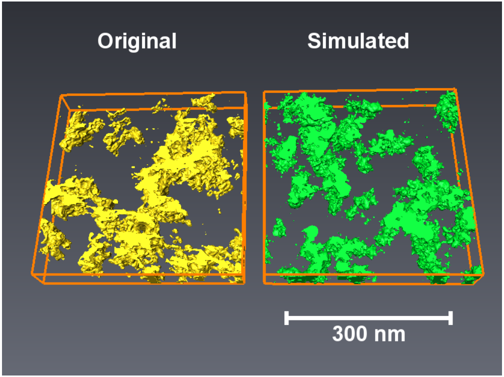

- Good visual agreement

Important structural characteristics for the morphology

- Spherical contact distribution function (probability of a random polymer voxel to find the ZnO phase within a given distance)

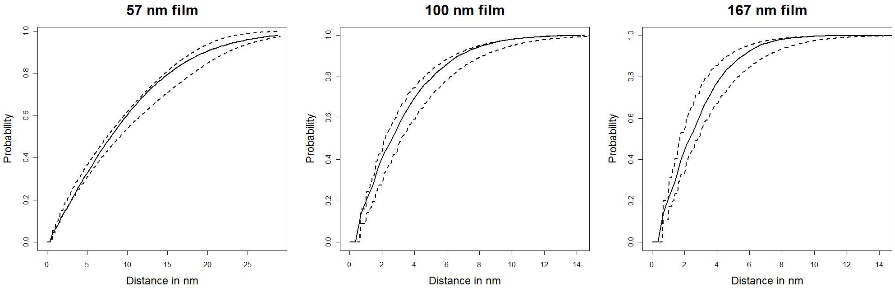

Distribution functions; solid lines: simulations; dashed lines: lower & upper bounds from original data.

Important structural characteristics for the morphology

- Volume fraction
- Connectivity (existence of percolation pathways to electrodes)

		Volume fraction	Connectivity (monotonous)
57 nm	model	0.115	0.887
	data	0.133	0.928
100 nm	model	0.216	0.888
	data	0.211	0.910
167 nm	model	0.210	0.809
	data	0.210	0.851

Physical characteristic for model validation

Quenching probability η_Q (probability of a random exciton to reach the ZnO-phase)

- η_Q obtained from the field $\{n(x), x \in B^c\}$ of local exciton densities in the polymer phase

Physical characteristic for model validation

Quenching probability η_Q (probability of a random exciton to reach the ZnO-phase)

- η_Q obtained from the field $\{n(x), x \in B^c\}$ of local exciton densities in the polymer phase
- $\{n(x), x \in B^c\}$ computed by solving the steady-state diffusion equation

$$0 = \frac{dn(x)}{dt} = -\frac{n(x)}{\tau} + D\nabla^2 n(x) + g, \qquad x \in B^c,$$

D: diffusion constant, τ: exciton life time, g: rate of exciton generation

Physical characteristic for model validation

Quenching probability η_Q (probability of a random exciton to reach the ZnO-phase)

- η_Q obtained from the field $\{n(x), x \in B^c\}$ of local exciton densities in the polymer phase
- $\{n(x), x \in B^c\}$ computed by solving the steady-state diffusion equation

$$0 = \frac{dn(x)}{dt} = -\frac{n(x)}{\tau} + D\nabla^2 n(x) + g, \qquad x \in B^c,$$

  D: diffusion constant, τ: exciton life time, g: rate of exciton generation
- boundary condition: $n(x) = 0$ for all $x \in \partial B^c \setminus \partial W$.

Physical characteristic for model validation

Quenching probability η_Q (probability of a random exciton to reach the ZnO-phase)

- η_Q obtained from the field $\{n(x), x \in B^c\}$ of local exciton densities in the polymer phase
- $\{n(x), x \in B^c\}$ computed by solving the steady-state diffusion equation

$$0 = \frac{dn(x)}{dt} = -\frac{n(x)}{\tau} + D\nabla^2 n(x) + g, \qquad x \in B^c,$$

  D: diffusion constant, τ: exciton life time, g: rate of exciton generation
- boundary condition: $n(x) = 0$ for all $x \in \partial B^c \setminus \partial W$.
- $\eta_Q = 1 - \bar{n}/(\tau g)$

Physical characteristic for model validation

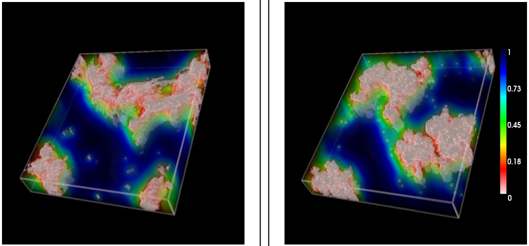

Real data

Simulated data

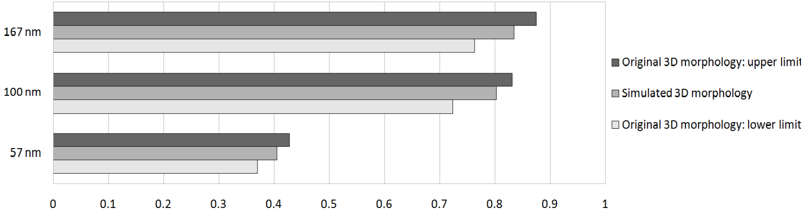

Model for morphology

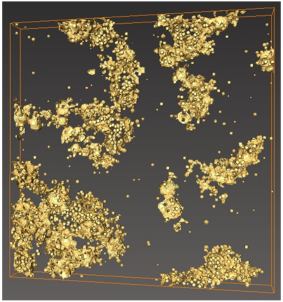

validated by
3D real image data

Model for transport processes

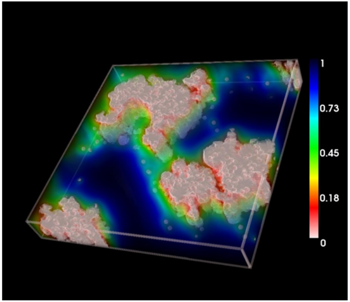

validated by
physical experiments

Virtual Material Design

Virtual material design

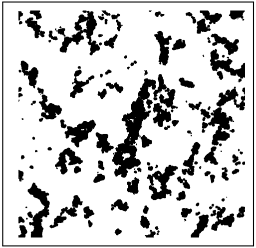

$\overset{\text{Model}}{\Longleftrightarrow}$ $$\vec{\lambda} = (\lambda_1, \ldots, \lambda_m)$$

Stochastic simulation model

$\Rightarrow$ 3D morphology represented by parameter vector $\vec{\lambda}$

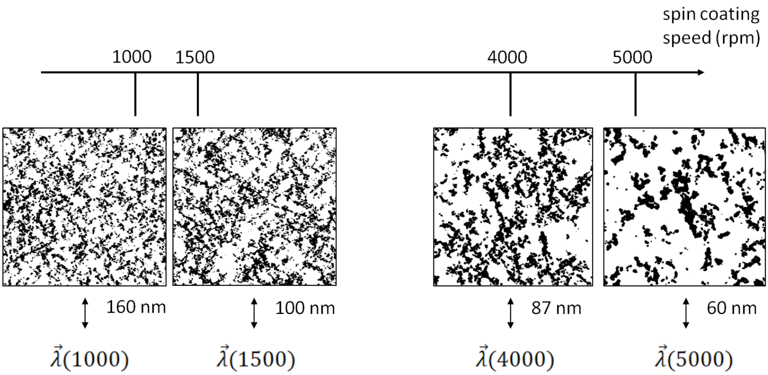

Spin coating speed determines morphology

- Regression of parameter vector $\vec{\lambda}$ allows prediction of morphologies which were not fabricated
- Manufacturing process can be realized virtually

Regression of model parameters

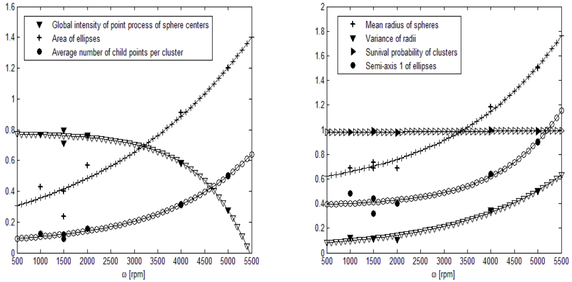

Spin coating speed determines morphology

- Regression models of type $\lambda_i(\omega) = a_i + b_i \exp(c_i\omega) + \varepsilon_i$ or $\lambda_i(\omega) = a_i + b_i\omega + \varepsilon_i$
- $\Rightarrow$ analytical formulae for $\vec{\lambda}$ in dependence of ω.
- Prediction of morphologies which were not fabricated

Scenario analysis

Model for layer thickness

- layer thickness $= c\omega^{\alpha},\ \alpha = -0.5$
- estimation of c by least squares
- simulation of virtual morphologies with ‘correct’ layer thickness

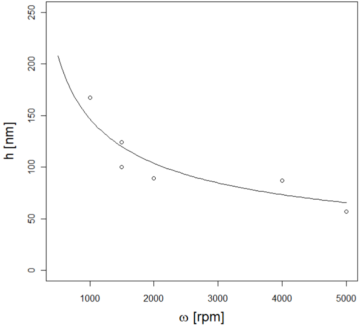

Scenario analysis

- Simulation of virtual morphologies for $\omega = 500, 750, \ldots, 5250$
- Estimation of structural and physical characteristics

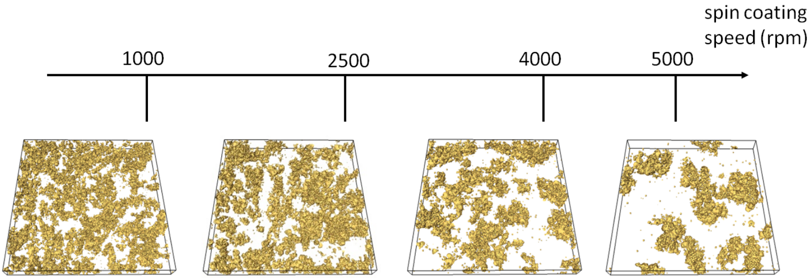

Scenario analysis - results

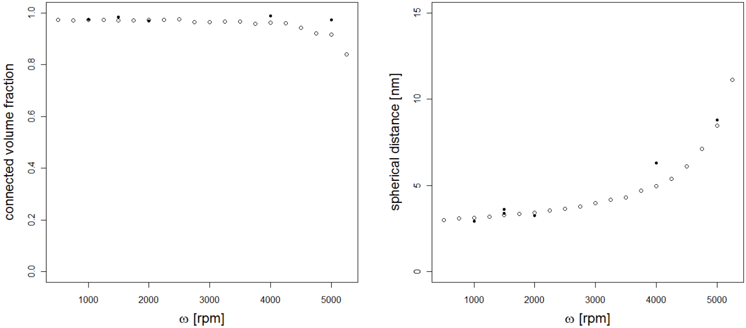

left: connectivity, right: mean spherical contact distance (in nm);
experimental data added by filled symbols

Scenario analysis - results

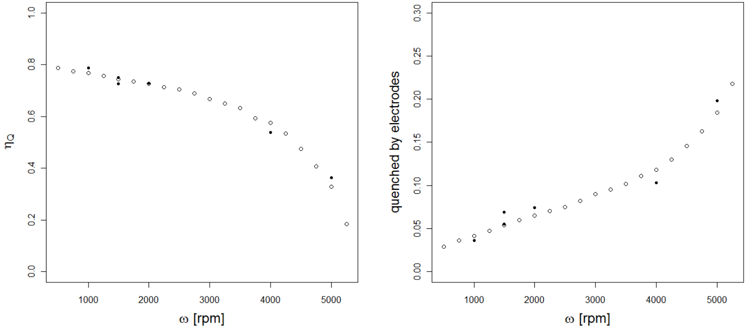

left: quenching efficiency by bulk, right: quenched by electrodes; experimental data added by filled symbols

3D patterns on microscopic scales

- Li-ion batteries
- organic solar cells
- **fuel cells**
- polycristalline alloys

Modeling of non-woven GDL

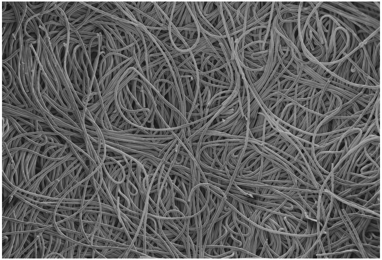

2D SEM image

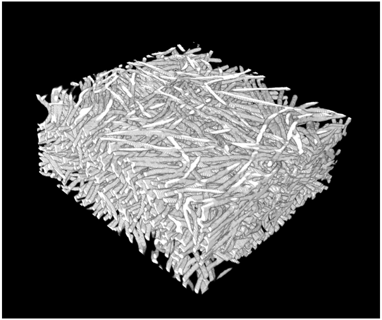

3D synchrotron data

Two different modeling approaches

- Multi-layer model

Modeling of non-woven GDL

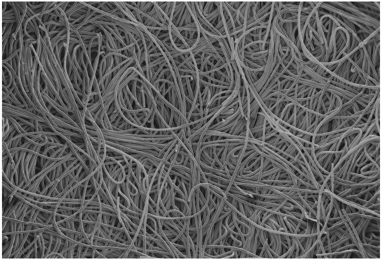

2D SEM image

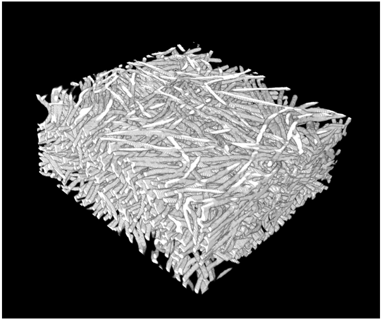

3D synchrotron data

Two different modeling approaches

- Multi-layer model
- Direct 3D modeling

Model assumptions

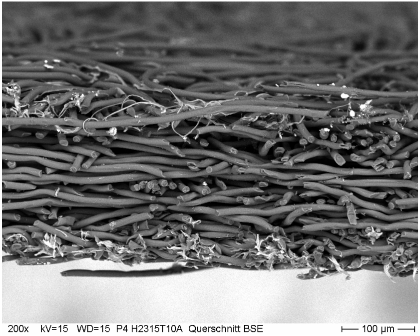

Cross section of non-woven GDL

- Horizontally oriented curved fibers

Model assumptions

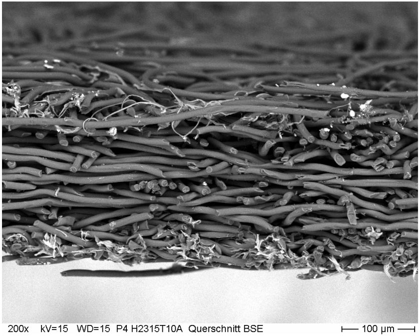

Cross section of non-woven GDL

- Horizontally oriented curved fibers
- GDL can be decomposed into independent thin horizontal layers

Model assumptions

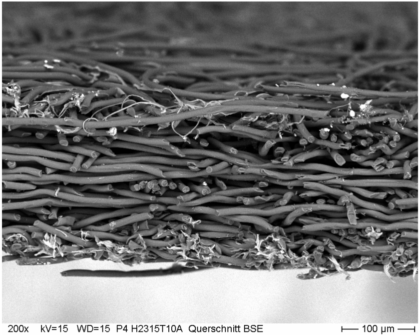

Cross section of non-woven GDL

- Horizontally oriented curved fibers
- GDL can be decomposed into independent thin horizontal layers
- Mutually penetrating fibers

Construction of 3D multi-layer model

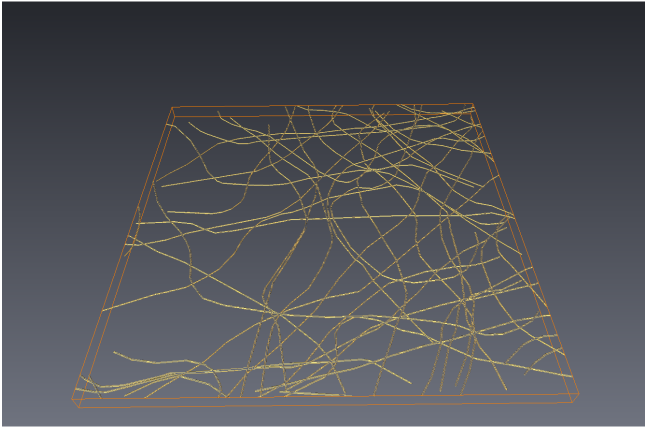

2D fiber model

Multi-Layer model

- Fiber model

Construction of 3D multi-layer model

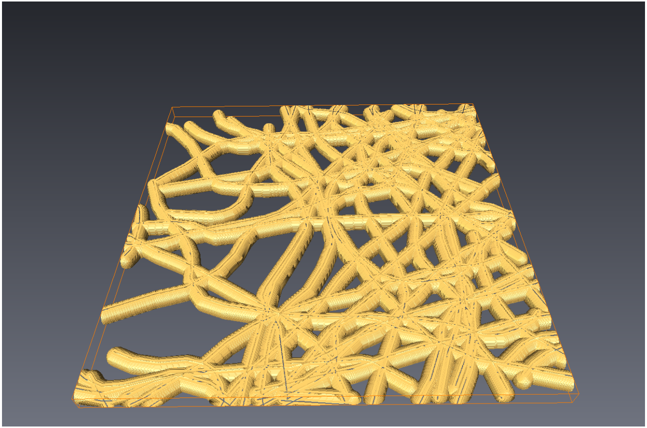

3D–dilation

Multi-Layer model

- Fiber model
- 3D–dilation

Construction of 3D multi-layer model

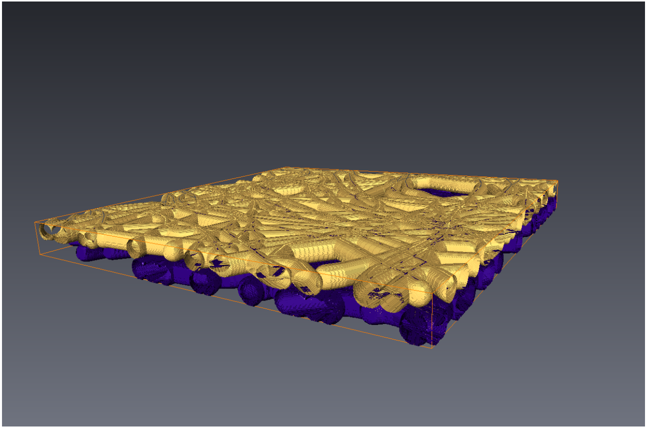

2 layers

Multi-Layer model

- Fiber model
- 3D–dilation
- More layers ...

Validation of 3D multi-layer model

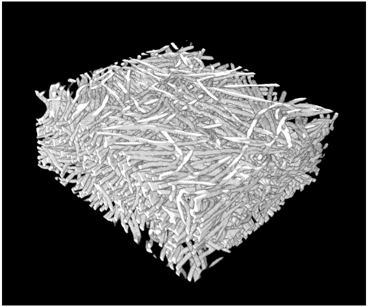

3D synchrotron data

Realization of multi-layer model

Goodness of fit

- Visual inspection

Validation of 3D multi-layer model

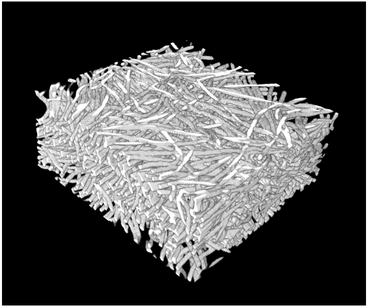

3D synchrotron data

Realization of multi-layer model

Goodness of fit

- Visual inspection
- Formal model validation

Discussion – multi-layer model

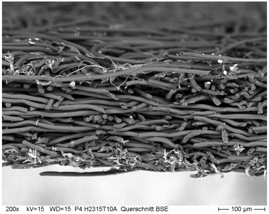

Cross section of GDL

Advantage

- Model fitting based on 2D SEM images

Discussion – multi-layer model

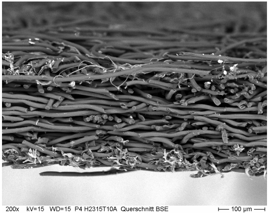

Cross section of GDL

Advantage

- Model fitting based on 2D SEM images
- Short run times

Disadvantage

- Fibers mutually penetrate

Discussion – multi-layer model

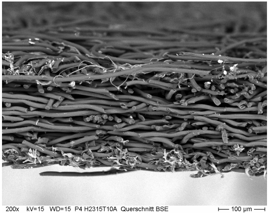

Cross section of GDL

Advantage

- Model fitting based on 2D SEM images
- Short run times

Disadvantage

- Fibers mutually penetrate
- Fibers have no gradient in z-direction

Goals

- Extraction of single fibers from 3D image data

Goals

- Extraction of single fibers from 3D image data
- Stochastic modeling of single fibers

Goals

- Extraction of single fibers from 3D image data
- Stochastic modeling of single fibers
- Construction of stochastic 3D model

Goals

- Extraction of single fibers from 3D image data
- Stochastic modeling of single fibers
- Construction of stochastic 3D model
- Validation of stochastic 3D model

Goals

- Extraction of single fibers from 3D image data
- Stochastic modeling of single fibers
- Construction of stochastic 3D model
- Validation of stochastic 3D model
- Modeling of PTFE

Stochastic connection algorithm

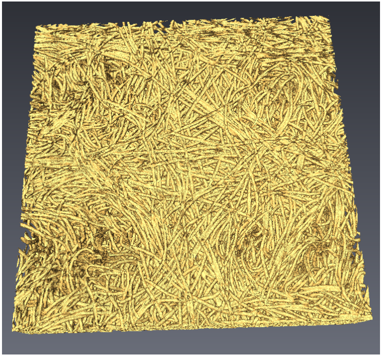

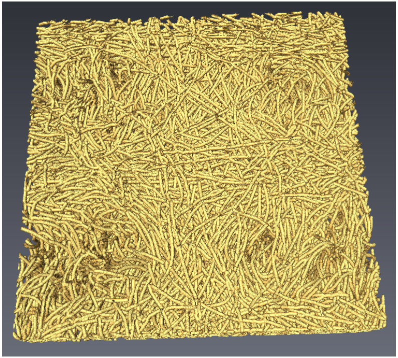

Left: original fibers

Right: extracted fibers

Validation by visual inspection

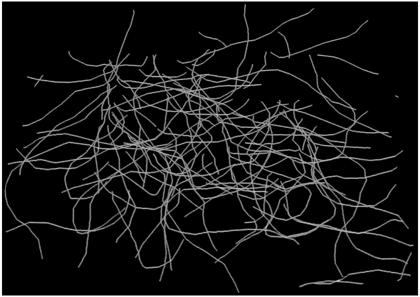

Extracted single fibers

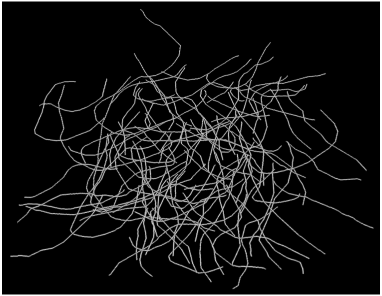

Realizations of single fiber model

Formal validation of vectorial time series model

Basic idea

- Monte-Carlo simulation of time series

Formal validation of vectorial time series model

Basic idea

- Monte-Carlo simulation of time series
- Transformation into polygonal tracks

Formal validation of vectorial time series model

Basic idea

- Monte-Carlo simulation of time series
- Transformation into polygonal tracks
- Comparison of geometric properties of extracted and simulated polygonal tracks

Formal validation of vectorial time series model

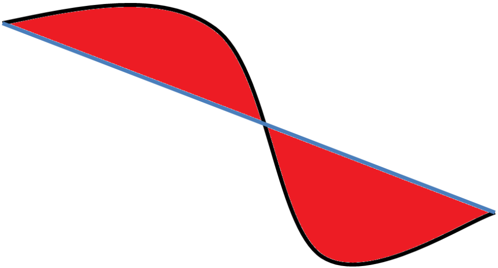

Measure for the amount of curvature: Volume of red area / (length of blue line)^2

Formal validation of vectorial time series model

Curvature properties of single fibers

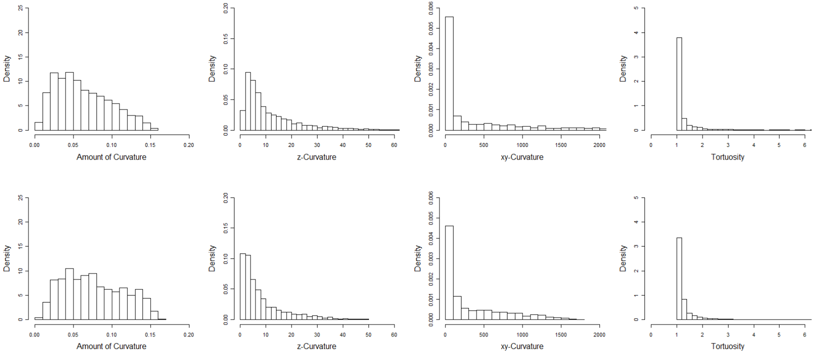

First row: Extracted polygonal tracks
Second row: Simulated polygonal tracks

Idea of 3D GDL model

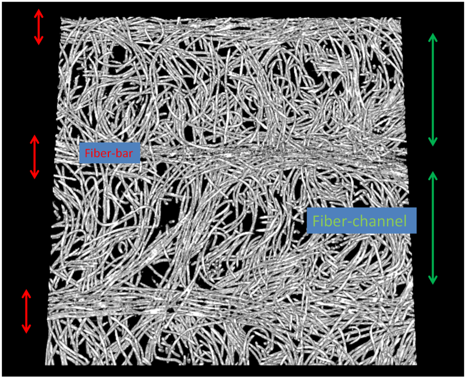

Cut-out of 3D synchrotron data

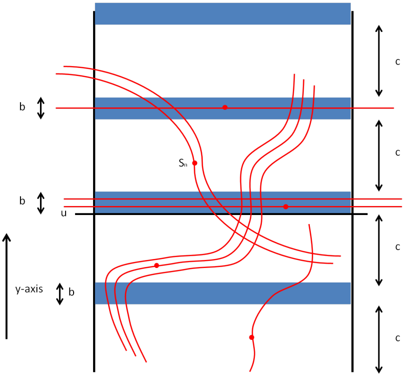

Basic idea of bar/channel modeling

Stochastic 3D GDL model

- A priori information
  - Radius of fibers: $r = 4.75\mu m$
  - Fiber length: $l = 50mm$
  - Volume fraction of fibers: 0.235
  - fiber-channel width $c = 500\mu m$
  - fiber-bar width $b = 70\mu m$

Stochastic 3D GDL model

- A priori information
  - Radius of fibers: $r = 4.75\mu m$
  - Fiber length: $l = 50mm$
  - Volume fraction of fibers: 0.235
  - fiber-channel width $c = 500\mu m$
  - fiber-bar width $b = 70\mu m$
- 3D GDL model
  1. $U \sim U[0, 570]$

Stochastic 3D GDL model

- A priori information
  - Radius of fibers: $r = 4.75\mu m$
  - Fiber length: $l = 50mm$
  - Volume fraction of fibers: 0.235
  - fiber-channel width $c = 500\mu m$
  - fiber-bar width $b = 70\mu m$
- 3D GDL model
  1. $U \sim U[0, 570]$
  2. Boolean model: $\Xi = \bigcup_{n=1}^{\infty} (B_n + S_n)$,
     - $\{S_n\}$ is a 3D Poisson process with intensity λ
     - B_n is the single bundle model of length l if $S_n \in$ fiber-channel, i.e., $S_n \in [u + i(b + c) - c, u + i(b + c)),\ i \in \mathbb{Z}$,
     - B_n is a line segment of length l parallel to the x-axis if $S_n \in$ fiber-bar, i.e., $S_n \in [u + i(b + c), u + i(b + c) + b),\ i \in \mathbb{Z}$

Stochastic 3D GDL model

- A priori information
  - Radius of fibers: $r = 4.75\mu m$
  - Fiber length: $l = 50mm$
  - Volume fraction of fibers: 0.235
  - fiber-channel width $c = 500\mu m$
  - fiber-bar width $b = 70\mu m$
- 3D GDL model
  1. $U \sim U[0, 570]$
  2. Boolean model: $\Xi = \bigcup_{n=1}^{\infty} (B_n + S_n)$,
     - $\{S_n\}$ is a 3D Poisson process with intensity λ
     - B_n is the single bundle model of length l if $S_n \in$ fiber-channel, i.e., $S_n \in [u + i(b+c) - c, u + i(b+c)),\ i \in \mathbb{Z}$,
     - B_n is a line segment of length l parallel to the x-axis if $S_n \in$ fiber-bar, i.e., $S_n \in [u + i(b+c), u + i(b+c) + b),\ i \in \mathbb{Z}$
  3. Dilate fibers with a 3D sphere: $\Xi \oplus B(0, r)$

Visual inspection of 3D GDL model

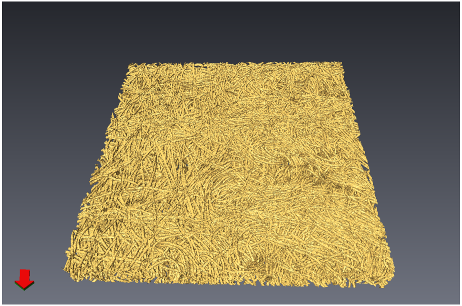

3D synchrotron data

Visual inspection of 3D GDL model

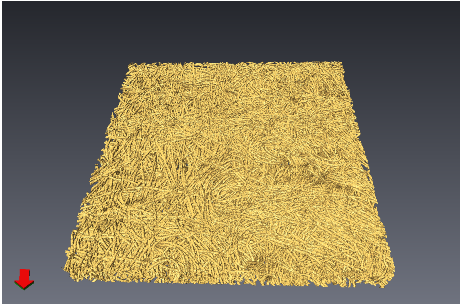

3D synchrotron data

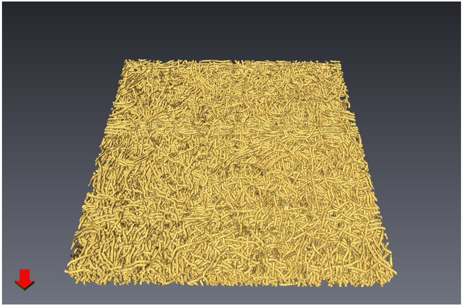

Simulated non-woven GDL drawn from the GDL model

Visual inspection of 3D GDL model

Alternative visualisation (with different choice of colors)

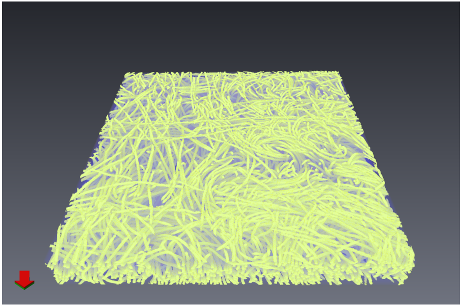

3D synchrotron data

Visual inspection of 3D GDL model

Alternative visualisation (with different choice of colors)

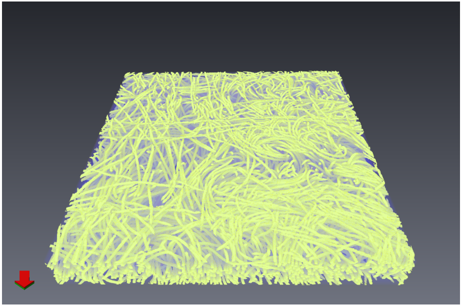

3D synchrotron data

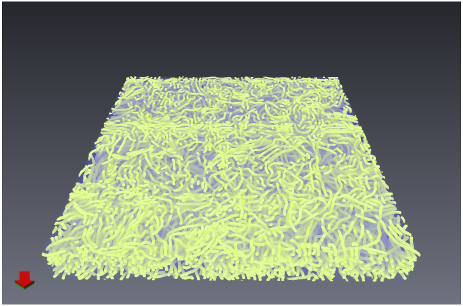

Simulated non-woven GDL drawn from the GDL model

Validation of 3D GDL model

Model validation using structural characteristics

- spherical contact distribution function (probability of a random pore voxel to reach the fiber phase within a given distance)

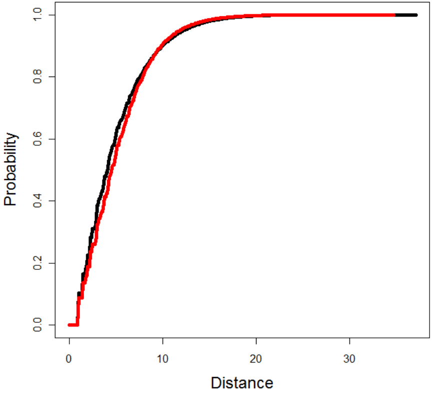

black: real GDL
red: simulated GDL

Validation of 3D GDL model

Model validation using structural characteristics

- spherical contact distribution function (probability of a random pore voxel to reach the fiber phase within a given distance)
- directional distribution of line segments

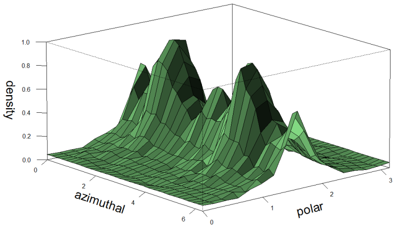

real GDL

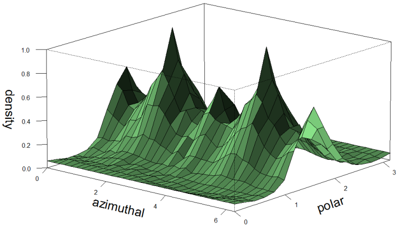

simulated GDL

Validation of 3D GDL model

Model validation using physical characteristics

- effective tortuosity (distribution of path lengths through a porous material)

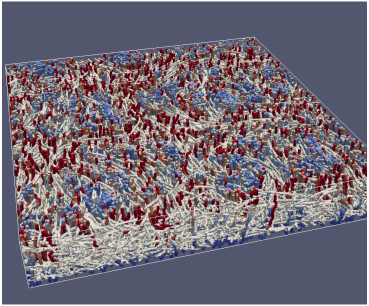

path lengths through real GDL

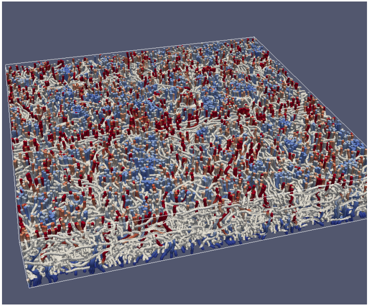

path lengths through simulated GDL

blue colored: short paths
red colored: long paths

Validation of 3D GDL model

Model validation using physical characteristics

- effective tortuosity (distribution of path lengths through a porous material)

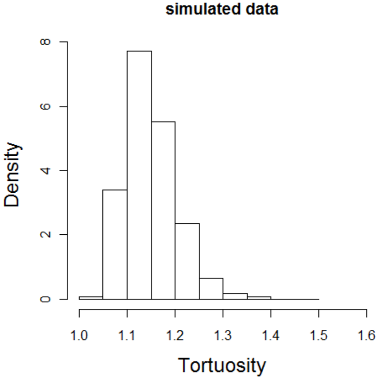

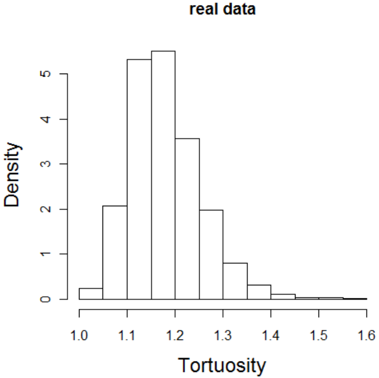

mean = 1.19 (real GDL) resp. mean = 1.15 (sim. GDL)

3D patterns on microscopic scales

- Li-ion batteries
- organic solar cells
- fuel cells
- **polycristalline alloys**

Alloys

- 3D morphology of eutectic Si corals in an Al matrix (left) and corresponding skeletonization (right)

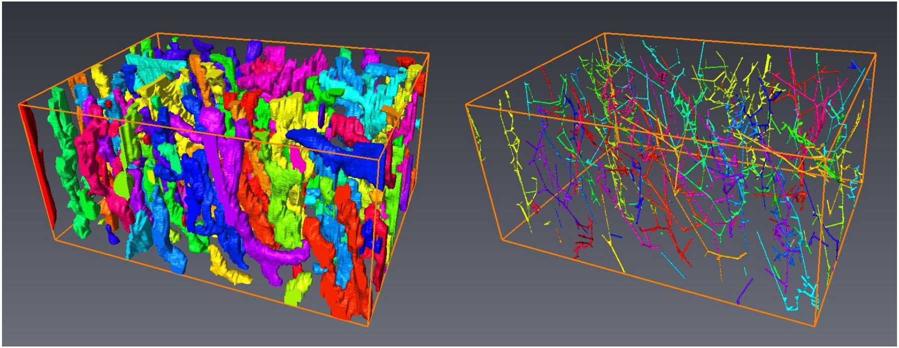

image size is $548 \times 761 \times 357$ voxel with voxel size of $46nm$

Alloys

- 3D skeletonization of Si corals (left) and corresponding stems (right)

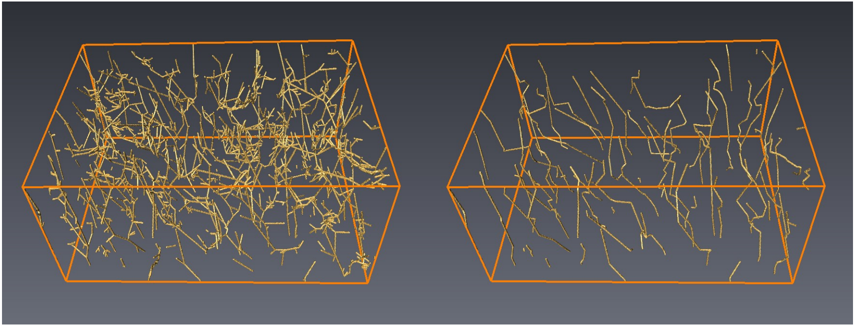

Alloys

Modeling idea of single coral:

- First the main stem is described by a random polygonal track where the endpoints of these line segments are numbered serially (0)
- Branches are added to the stem and numbered serially ((1), (2)) and
- finally branches are deleted ((3), red colored) which are too close to each other

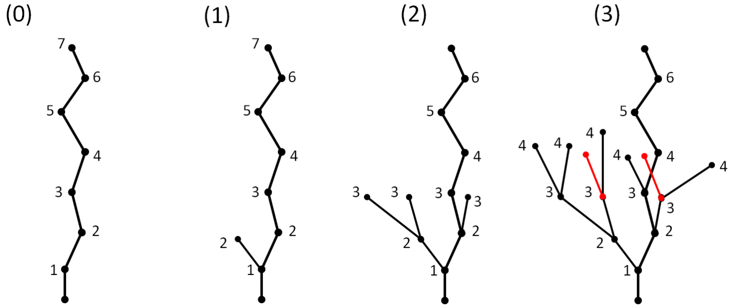

Alloys

- 3D graph structure of Si corals in an Al matrix (left) and realization of the stochastic model for aggregates of corals (right)

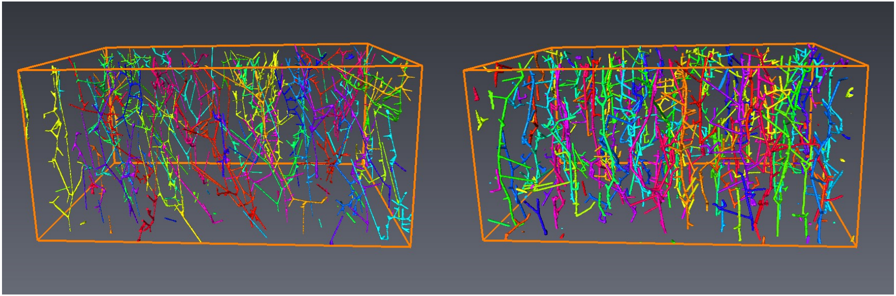

Alloys

- spherical contact distribution function (left), distribution of edge lengths (center) and distribution of maximum stem length (right)
- black: computed for the graph structure of experimental Si corals, red: drawn from the multi-coral model

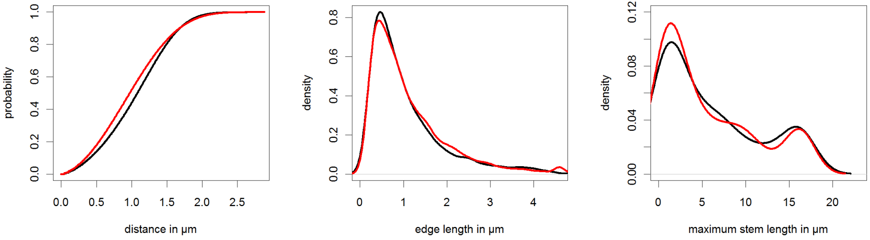

Alloys

- 3D morphology of experimental Si corals in an Al matrix (left) and corresponding simulation of stochastic model (right)

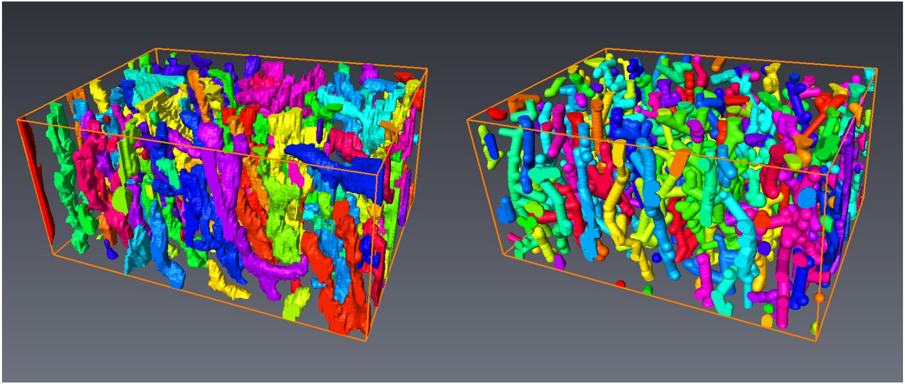

image size is $761 \times 548 \times 357$ voxel with voxel size of $46nm$

Alloys

- Distribution of spherical contact distances from Al to Si particles (left), and vice versa (right) for the experimental image data (black curve) and realization drawn from the stochastic model (red curve)